4-1-1993

Conversion of solid ink density and dot gain specifications into colorimetric specifications

Theera Tangvichachan

Conversion of Solid Ink Density and Dot Gain Specifications into Colorimetric Specifications

by

Theera Tangvichachan

A thesis submitted in partial fulfillment of the
requirements for the degree of Master of Science in the
School of Printing Management and Sciences in the College
of Imaging Arts and Sciences of the Rochester Institute of Technology

April 1993

Thesis Advisor: Mr. Franz Sigg
Research Advisor: Mr. J. A. Stephen Viggiano

School of Printing Management and Sciences
Rochester Institute of Technology
Rochester, New York

Certificate of Approval

Master's Thesis

This is to certify that the Master's Thesis of

Theera Tangvichachan

With a *major in Printing Technology*
has been approved by the Thesis Committee as satisfactory
for the thesis requirement for the Master of Science degree
at the convocation of

April 1993

Thesis Committee:

Franz Sigg
Thesis Advisor

Joseph L. Noga
Graduate Program Coordinator

George H. Ryan
Director of Designate

Conversion of Solid Ink Density and Dot Gain Specifications into Colorimetric Specifications

I, Theera Tangvichachan, hereby **grant permission** to the Wallace Memorial Library of the Rochester Institute of Technology to reproduce my thesis in whole or in part. Any reproduction will not be for commercial use or profit.

April, 1993
Date

Signature of Author

The virtue of this thesis is attributed to my parents, pedagogues, kin, and friends.

Acknowledgments

Firstly, I would like to express my appreciation to the Royal Thai Government for providing the financial support throughout my study at R.I.T. My special gratitude is conveyed to Mr. Franz Sigg for being an encouraging, giving, and knowing Thesis Advisor. Mr. Stephen Viggiano, my Research Advisor, is deeply appreciated for allowing me to employ his computer programs and for spending his valuable moments in explaining how they perform. Finally, I also thank Professor Robert Chung for sharing his knowledge of the JMP program and Professor Joseph Noga for assisting in the academic affairs during the past two years. With all their help and support, my study at R.I.T. came to completion.

Table of Contents

List of Tables

Table

List of Figures

Figure

Abstract

With the advent of the spectrophotometer as an alternative to the densitometer for pressroom applications, it becomes desirable to use a single three-color overprint halftone gray patch for controlling color on the press. As a consequence, the need for new specifications in colorimetric units, rather than SID and dot gain units, arises. The purpose of this study was to conduct a mathematical conversion of the traditional SID and dot gain specifications into the colorimetric specifications, in terms of the CIELAB coordinates.

The FIPP dot gain and SID specifications were applied to the gray patch contained in the Gretag CMS3 color control bar. This gray comprises an overprint of 75% cyan, 62% magenta, and 60% yellow. Applying all possible SID and dot gain tolerances to this gray results in overall 225 three-color overprint grays. By employing computer programs containing the GRL Trapping Model, (2) the GRL Dot Gain Model, and (3) the Yule-Nielsen modified Spectral Neugebauer Model, the CIELAB coordinates of the 225 grays were predicted without taking actual spectrophotometric measurements on press sheets. The CIELAB coordinates of these grays were then plotted in the three-dimensional L* a* b* space. The shape of the cluster of these 225 grays is nearly spherical. The largest deviation of one of

these grays from the aim gray is 4.7 ΔE^*_{ab} units. Varying any dot area by ± 2% or changing any SID by ± 0.1 causes a color deviation of less than 3 ΔE^*_{ab} units.

Chapter 1

Introduction

> Colour, . . . , involves not only material sciences, such as physics and chemistry, but also biological sciences, such as physiology and psychology; and, in its applications, colour involves various applied sciences, such as architecture, dyeing, paint technology, and illuminating engineering.[1]

Color perception is a complex phenomenon influenced by physiological, psychological, and physical factors.[2] That a color can be differently perceived by different observers with different color visions and experiences is associated with the physiological and psychological aspects. As a physical phenomenon, color appearance involves (1) a source of light, (2) an object to modify the illuminating light, and (3) an observer to sense the stimulus.

In a color printing process, a considerable number of variables affect reproduced colors on a press. Of all these variables, the most two significant are solid ink density (SID) and dot gain. To maintain high quality and consistency in color reproduction throughout a press run, SID and dot gain have to be measured and then controlled so that color variations caused by changes of these two variables are kept at a minimum.

Statement of the Problem

Old and New Methods of Color Control in Printing

Colors that are reproduced in the lithographic printing process are achieved by printing and overprinting the various sizes of process ink dots. In order to optimize a color reproduction, printers attempt to control solid ink density and the amount of dot gain and to keep them close to aim values within the standardized tolerances. Traditionally, they evaluate printed colors by (1) visual assessment and/or (2) taking measurements with a densitometer. Colored images on a press sheet are visually evaluated and compared to those on the OK press or proof sheet under a specific viewing condition. Because color sensation is governed by the earlier-mentioned psychological and physiological factors, the visual assessments of colors by human observers are prone to vary from time to time and from one observer to another. Since visual assessment is subjective and qualitative, but not quantitative, "objective" measurement methods are required to compliment visual assessment. A densitometer that is designed to read SID and apparent dot area of printed colored images has been used to serve this objective requirement. As a tool for process control where printers only want to make sure that all press sheets are alike, densitometers function very effectively. In addition, they have the advantage that they are relatively inexpensive and simple to use. However, they do not respond to colors in the same manner as the human eye does.

There are two types of instruments that respond to colors like the human eye does: the spectophotometer and the colorimeter. Recently, they have become available as an alternative to densitometers for applications of color measurements in the graphic arts. Therefore, the need arises for new printing standards and specifications of tolerances in colorimetric units, rather than in units of SID and dot gain.

Aspects of Conventional Color Control in Printing

In order to optimize tone and color reproduction on a press, all that printers can adjust is ink film thickness (IFT). They try to control IFT (therefore color) by controlling SID of each printed process ink. A control of only SID, however, is not enough since the sizes of halftone dots can change when inks are transferred from a printing plate to a substrate. The growth of halftone dot size from dot on a film to dot on a printed sheet is called dot gain. The occurrence of dot gain is influenced by printing pressures, rheological properties of the inks, types of papers, and screen rulings. Dot gain is therefore a variable that needs to be controlled even though printers have only limited and indirect control over it.

Many people experimented with SID and dot gain and then came up with company standards, national standards, and international standards.

Standardized Tolerances for Solid Ink Density and Dot Gain

In order to optimize color reproduction, printers control colors on a press sheet in accordance with specifications and tolerances for SID and dot

gain. Those specifications and tolerances are set forth by a number of associations or organizations of the printing industry, for example, FIPP (International Federation of the Periodical Press)[3], FOGRA (German Research Association for Printing and Reproduction Technology)[4], and Gretag.[5] The SID and dot gain tolerances issued by FIPP, FOGRA, and Gretag are summarized and compared in Tables 1 and 2.

Table 1

FIPP, FOGRA, and Gretag aim solid ink densities on coated paper

Type of Filter	Cyan			Magenta			Yellow		
	Fp(1)	Fg(2)	Gr(3)	Fp	Fg	Gr	Fp	Fg	Gr
Narrow-band, polarized	1.40	–	1.45	1.50	–	1.40	1.40	–	1.40
Narrow-band, nonpolarized	1.20	–	–	1.30	–	–	1.20	–	–
Broad-band, polarized	1.30	–	1.45	1.40	–	1.40	1.10	–	1.00
Broad-band, nonpolarized	1.20	–	–	1.30	–	–	1.00	–	–

Note: (1) The FIPP (Fp) SID tolerance of - 0.0 to + 0.2 is allowable. The deviations should be uniformly high or low for all colors.

(2) FOGRA (Fg) does not recommend absolute aim SID figures. However, the indice of mean (aim) SID tolerance are given to calculate the deviations of the mean. The index of the mean SID tolerance for production run is $\pm$ 8%, for example, tolerance for SID of 1.4 is $\pm$ 0.11 which is the same as the Gretag and FIPP specifications. The procedures to attain the absolute SID tolerances are contained in the FOGRA Praxis Report No. 30.

(3) The Gretag (Gr) SID tolerance for all colors is ± 0.10 except that the tolerance of yellow SID read with a broad-band, polarized blue filter is ± 0.05. The grey balance patch should be a neutral gray, which is another way of saying that the deviations within tolerances should be uniformly high or low.

Table 2

FIPP, FOGRA, and Gretag dot gain specifications for printing at 150 line screen on coated paper and with positive-working plates

	Percent Dot Gain					
	FIPP[1]		FOGRA		Gretag[2]	
Tint	Aim (%)	Tolerance (%)	Aim (%)	Tolerance (%)	Aim (%)	Tolerance (%)
40%	18	± 2	18	± 3	14, 16	± 3
50%	19	± 2	–	–	–	–
70%	16	± 2	–	–	–	–
75%	14	± 2	–	–	–	–
80%	12	± 2	11	± 2	9, 10	± 2

Note: (1) The dot gain in Cyan, Magenta, and Yellow should be uniformly high or low

(2) The aim dot gain values in both Cyan and Magenta are 14% at 40% tint and 9% at 80% tint. The aim dot gain values in Yellow is 16% at 40% tint and 10% at 80% tint. The grey balance patch should be a neutral gray, which is another way of saying that the deviations within tolerances should be uniformly high or low.

In order to understand how the SID and dot gain tolerances affect tone and color reproductions of printed images, printers have to select some colors

and monitor how they are affected by those tolerances. Traditionally dot areas between 40% and 80% have been used to evaluate and control dot gain. However, with the application of colorimetry, a single color patch can be used to accomplish the same task. It is evident that a single gray is an excellent choice to serve this purpose.

Three-Color Overprint Gray for Detection of Color Variation in Printing

Neutral areas of any image are referred to the areas of hueless, or achromatic colors being comprised of every degree of grayness from white to black. It is essential that the neutral areas of an original be reproduced as a neutral gray without any evident color cast of printed images. If this criterion is not fulfilled, a color cast will take place in the entire color reproduction process. Due to their achromaticity, neutral grays are the most suitable printed areas for monitoring color variation. To achieve a true neutral gray, it is necessary to print larger dot areas of cyan ink than those of magenta and yellow inks. The CMY dot area combinations for gray balance achievement, that are addressed by FIPP, FOGRA, and Gretag, are listed in Table 3.

In order to decide which gray level should be used to control the press, an actual scenario of what happens on the press has to be considered.

At the beginning of a press run, the amount of dot gain is low because the press is still cold. After a number of impressions, the press starts warming up. When temperature increases, ink viscosity and ink tack will decrease. As a result, dot gain increases. Because maximum dot gain occurs

Table 3

Determination of Gray Balance recommended by FIPP, FOGRA, and Gretag

	Halftone Dot Area		
	Cyan	Magenta	Yellow
FIPP	50%	38–42%	38–42%
FOGRA (a)	28%	21%	19%
(b)	75%	63%	60%
Gretag CMS3	75%	62%	60%

Note: The FOGRA CMY dot area combination of (a) produces gray equivalent to 40% black tint whereas the FOGRA CMY dot area combination of (b) produces gray equivalent to 80% black tint.

in the middletone areas (See Figure 1), maintaining proper middletone dot gain would require a drastic lowering of SID. An excessive reduction of SID to compensate for dot gain on the press will certainly negatively affect tone reproduction, shorten reproducible color gamut, decrease vividness of printed colors, and lessen contrast of the printed images. Therefore, keeping a three-quarter tone constant (rather than a middletone or a solid) means making a practical compromise between the middletone that is too dark and the solid that is too light.

For this reason, it makes sense to use a dark gray to control tone reproductions on a press. Therefore, the gray balance of Gretag CMS3, which is in agreement with FOGRA, is adopted to be an aim gray in this study.

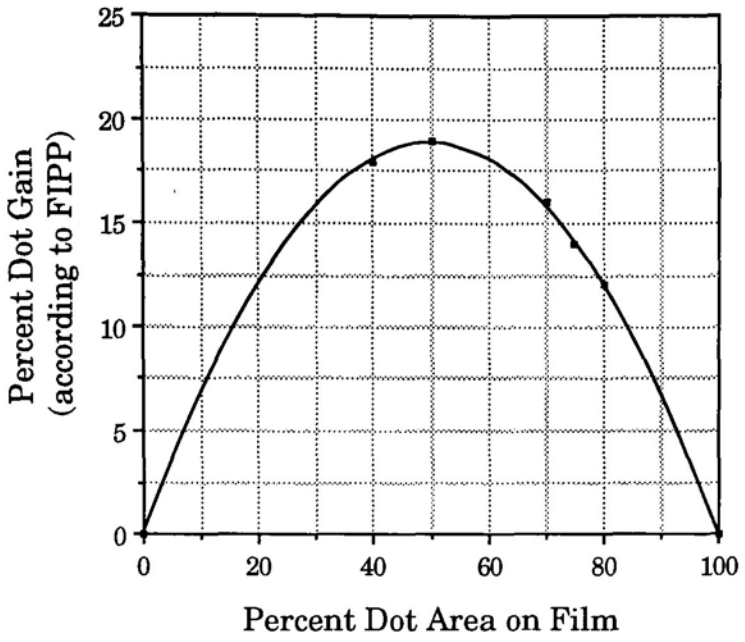

Figure 1. Dot gain curve illustrates the highest amount of dot gain at the middletone areas. Percent dot area on film is plotted against percent dot gain specified by FIPP for printing at 150 line-per-inch screen with a positive-working plate on a coated paper.

Applied Colorimetry for Color Control in Pressroom

Colorimetry is a science of quantifying and specifying the visual appearance of color directly corresponding to the spectral sensitivities of human perception. Such a system was first developed in 1931 by the Commission Internationale de l'Èclairage (CIE). After 1931, the CIE system has been mathematically improved to achieve perceptual uniformity. One of the CIE Uniform Color Spaces widely used and well known is the CIELAB system.

There are two types of instruments that permit colorimetric measurements; the colorimeter and the spectrophotometer. The tristimulus filter colorimeter is an instrument that has the combination of relative spectral power distribution of light source, spectral transmittances of filters and relative spectral responses of photodetectors, simulating the color matching functions of the CIE Standard Observers.[6] It quantifies a color in terms of tristimulus values X, Y, Z or L*, a*, b* values. The spectrophotometer is an instrument used for determining spectral reflectance or transmittance of an object color, wavelength-by-wavelength. The spectral reflectance or transmittance data of the object are used for the calculations of the tristimulus values by a computer connected with the spectrophotometer.

The American National Standards Institute (ANSI) has defined the standard illumination with a correlated color temperature of 5000K (D_{50}) for viewing and appraising transparencies, proofs and press sheets. The spectrophotometer for the applications in the graphic arts industries is nowadays capable of measuring tristimulus values of a color viewed under the Illuminant D_{50}. The relative spectral power distribution and tristimulus values of the CIE illuminant D_{50} can be looked up in the CIE Publication No 15.2 (1986).

Objectives of the Study

This research will be conducted to answer the following questions:

(1) If SID and dot gain specifications are converted into the CIELAB coordinates, how do these tolerances appear in the CIELAB space?

(2) What is the maximum CIE ΔE^*_{ab} unit of these colorimetric tolerances ?

Endnotes for Chapter 1

[1]R. W. G. Hunt, "Colour Vision," in *Measuring Colour*, Ellis Horwood Series in Applied Science and Industrial Technology, 2d ed. (New York: John Wiley & Sons, 1987) , 21.

[2]Gary G. Field, "The Perception of Color," in *Color and Its Reproduction* (Pittsburgh, PA: Graphic Arts Technical Foundation, 1988), 23.

[3]International Federation of the Periodical Press (FIPP), *Specifications for European Offset Printing of Periodicals*, rev. 2d ed. (United Kingdom:International Federation of the Periodical Press, 1988).

[4]Deutsche Forschungsgesellschaft für Druck- und Reproduktionstechnik E.V. (FOGRA), *BVD/FOGRA Standardisation of Offset Printing*, FOGRA Praxis Report Nr. 30, rev. 2d ed. (Munich, West Germany: Deutsche Forschungsgesellschaft für Druck- und Reproduktionstechnik E.V, 1984).

[5]Gretag Company, *Gretag Sticker with Recommended Solid and Dot Gain Aim Values and Tolerances*, Gretag Product No. 98.16.75 KL8511 (Switzerland: Gretag Company, n.d.).

[6]Richard S. Hunter and Richard W. Harold, eds. , "Instruments for the Chromatic Attributes of Object Appearance," in *The Measurement of Appearance*, 2d ed. (New York: John Wiley & Sons, 1987) , 296-302.

Chapter 2

Theoretical Bases of the Study

In carrying through this study, the essential theoretical foundations, encompassing dot gain calculations, the CIE Color Measurement System, the Neugebauer Equations, and the extended Spectral Yule-Nielsen Equation, are clarified in this chapter.

Quantification of Dot Gain

Percent dot gain, that is a figure indicating the amount of the enlargement of halftone dot size from a film to a printed sheet, is derived from subtracting percent halftone dot area of a given area on film from that of a corresponding area on a press sheet. The apparent dot area (ADA), or effective dot area (EDA), on a press sheet is computed by employing the Murray-Davies equation:

$$\text{ADA} = \frac{1 - 10^{-Dt}}{1 - 10^{-Ds}} \times 100\% \tag{2.1}$$

where ADA is the apparent dot area, Dt is the density of the tint patch of the printed test target, and Ds is the density of the solid patch of the printed test target.

The apparent dot area calculated from the Murray-Davies equation incorporates both physical and optical dot areas. To exclude the optical influence from the computed apparent dot area, the Yule-Neilsen refined Murray-Davies equation is applied instead:

$$\text{PDA} = \frac{1 - 10^{-Dt/n}}{1 - 10^{-Ds/n}} \times 100\% \qquad (2.2)$$

where PDA is the physical dot area, Dt is the density of the tint patch of the printed test target, Ds is the density of the solid patch of the printed test target, and n is a correction factor compensating for optical dot gain.

Densitometers, which are extensively used as a tool for process control in the graphic arts industry, are not an applicable device for measuring color appearance. It is designed to denote numbers corresponding to the amount of light reflected from a press sheet; namely, to measure the light absorbance characteristics of colorants comprised in process inks, or corresponding to the amount of light transmitting through a piece of photographic film. In order to be able to detect and measure the amount of red, green, and blue light of the visible spectrum, densitometers are equipped with red, green, and blue filters. The spectral responses of the red, green, and blue channels of the densitometer do not exactly represent the spectral sensitivity of the human eye.[1] Figures 2 and 3 depict the spectral responses of the CIE Standard Observers [2] and the Status T [3] calibrated densitometer. Their spectral

sensitivity curves differ in location, width, and shape across the visible spectrum. Accordingly, it is apparent that the densitometer does not view a color in the same manner as the human eye does. Two colors with different hues plausibly have the same density readings even if they are perceived differently by the human eye. With this inherent restriction, the densitometer sees a color in an analogy to a person with an anomalous trichromat.[4] The capability of the densitometer in measuring a color was likewise expounded by Richard S. Hunter:[5]

> A densitometric measurement of a color is suitable for identification of the color only with the same instrument and colorant system. Methods of densitometry can be used for accurate color identification only within each single system of dyes and base materials. Thus densitometry does not have the broad ability of tristimulus colorimetry to identify color appearance regardless of materials used. On the other hand, densitometric measurements within a single system can provide precise separation of small color differences.

The CIE System for Color Measurement [6]

Prior to the period of a development of color measurement system, the artist Albert H. Munsell in 1905 originated a system for arranging colors. On the basis of the Munsell Color Notation, a color can be numerically described in terms of the three perceptual attributes: Hue, Value, and Chroma, e.g., 5G 8/10 is symbolized for a color possessing Hue of middle green, Value of 8, and Chroma of 10; namely, referred to a dark vivid green. Of all the three color attributes, hue is the most obviously perceptual attribute by

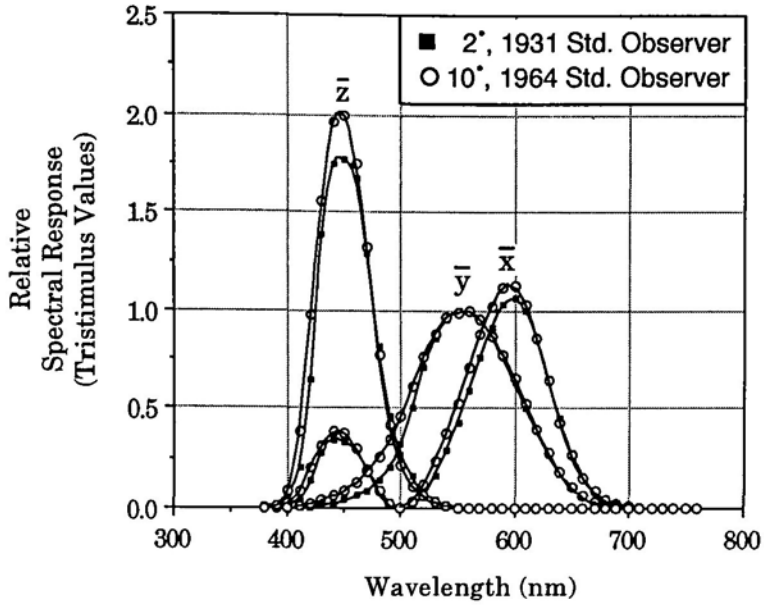

Figure 2. The color matching function curves for the 2° (1931) and supplementary 10° (1964) CIE Standard Observers delineate the representative spectral responses of the human eye.

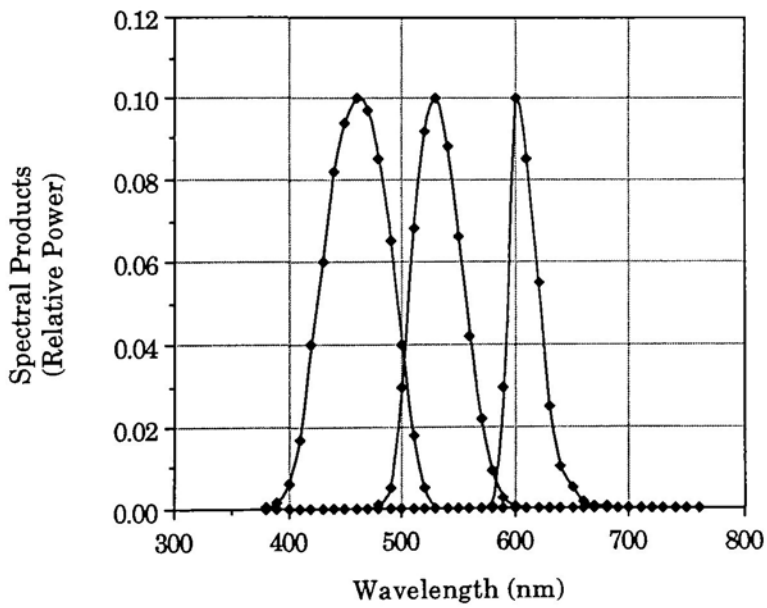

Figure 3. The Spectral Products (Status T Densities) curves illustrate the spectral responses of the Status T calibrated densitometer.

which an object color is called red, green, yellow, purple, and so forth. Chroma is a term designating the intensity of a color, its vividness, colorfulness, or deviation from gray. Unlike hue and chroma, value, or lightness, is an achromatic attribute of a visual sensation by which a white object is distinguished from gray and dark objects. It is therefore characterized according to the ability of a color to reflect or transmit the relative amount of light illuminating it.

In 1931, the Commission International de l'Éclairage (CIE) or International Commission on Illumination developed its system for color measurement. The CIE defined the standard illuminants and the standard observer. A color in the CIE system is specified by its tristimulus values. Tristimulus values X, Y, and Z of a color are the integral product of multiplying spectral reflectance factors of the object color with the spectral power distribution of the illuminant and with the color matching functions of the standard observer throughout the visible wavelengths as shown in the following equations:

$$X = k \int_{380}^{760} S(\lambda)\, R(\lambda)\, \bar{x}(\lambda)\, d\lambda \tag{2.3a}$$

$$Y = k \int_{380}^{760} S(\lambda)\, R(\lambda)\, \bar{y}(\lambda)\, d\lambda \tag{2.3b}$$

(2.3c) $$Z = k \int_{380}^{760} S(\lambda)\, R(\lambda)\, \bar{z}(\lambda)\, d\lambda$$

(2.3d) $$k = \frac{100}{\int_{380}^{760} S(\lambda)\, \bar{y}(\lambda)\, d\lambda}$$

where $S(\lambda)$ is spectral power distribution of a given illuminant or light source; $R(\lambda)$ is spectral reflectance factors of a colored object, $\bar{x}(\lambda)$, $\bar{y}(\lambda)$, $\bar{z}(\lambda)$ are 2° or 10° color matching functions of the standard observer; k is a normalizing factor for luminance; and $d\lambda$ is the wavelength interval. While the Y tristimulus value correlates with lightness, the X and Z tristimulus values do not correlate with perceptual color attributes, hue and chroma. The comparison in terms of hue and chroma differences from two different sets of tristimulus values X, Y, and Z is moreover meaningless because tristimulus values represent an ordinal scale. The CIE, hence, established the chromaticity coordinates x, y, and z which are mathematical transformations of the tristimulus values X, Y, and Z:

(2.4a) $$x = \frac{X}{X+Y+Z}$$

(2.4b) $$y = \frac{Y}{X+Y+Z}$$

(2.4c) $$z = \frac{Z}{X+Y+Z}$$

where x, y, and z are chromaticity coordinates and X, Y, and Z are tristimulus values. When the colors of the Munsell system are plotted in the CIE chromaticity diagram, the spacing of the Munsell loci shows a lack of uniformity. Because the Munsell system is based on equal visual differences, this lack of uniformity indicates that equal distances on the CIE chromaticity diagram do not represent equal visual difference.

One of the uniform color scales, that was developed in 1976 to improve the uniformity of visual perception of the CIE system, is the CIE L*a*b* system. The L*, a*, and b* figures are the result of a nonlinear, mathematical transformation of the tristimulus values X,Y, and Z. The establishment of the CIELAB color scale relies on the opponent color concept: the color that is perceived by the human eyes cannot be both light and dark at the same time, both red and green at the same time, or both yellow and blue at the same time. The lightness in the CIELAB color scale is symbolized with L*, redness and greenness are expressed as +a* and -a* respectively, and yellowness and blueness are defined as +b* and -b* respectively. The L* a* b* values are calculated by the following equations:

(2.5a) $$L^* = 116 \cdot F(Y) - 16$$

(2.5b) $$a^* = 500[F(X) - F(Y)]$$

(2.5c) $$b^* = 200[F(Y) - F(Z)]$$

where:

(2.6a) $$F(X) = (X/Xn)^{1/3} \quad \text{when} \quad X/Xn > 0.008856$$

(2.6b) $$F(X) = 7.787(X/Xn)^{1/3} + 0.1379 \quad \text{when} \quad X/Xn \leq 0.008856$$

(2.6c) $F(Y) = (X/Xn)^{1/3}$ when $Y/Yn > 0.008856$

(2.6d) $F(Y) = 7.787(X/Xn)^{1/3} + 0.1379$ when $Y/Yn \leq 0.008856$

(2.6e) $F(Z) = (Z/Zn)^{1/3}$ when $Z/Zn > 0.008856$

(2.6f) $F(Z) = 7.787(Z/Zn)^{1/3} + 0.1379$ when $Z/Zn \leq 0.008856$

where X, Y, and Z are tristimulus values of the given color and X_n,Y_n, and Z_n are tristimulus values of the illuminant or the reference white (referred to paper in this study).

In the CIELAB system, the other two useful parameters are Psychometric Chroma (C^*_{ab}) and Psychometric Hue Angle ($h°_{ab}$). C^*_{ab} and $h°_{ab}$ are derived from a* and b* by the following equations:

(2.7a) $$C^*_{ab} = [(a^*)^2 + (b^*)^2]^{1/2}$$

(2.7b) $$h°_{ab} = \arctan (b^*/a^*)$$

Color variation between a sample color and a standard color is determined by the CIELAB color difference (ΔE^*_{ab}) figure which indicates how much a sample differs in chroma, hue, and lightness from a standard. To calculate the color difference, the following equation is used:

(2.8) $$\Delta E^*_{ab} = [(\Delta L^*)^2+(\Delta a^*)^2+(\Delta b^*)^2]^{1/2}$$

where ΔE^*_{ab} is the total perceived color difference and ΔL^*, Δa^*, and Δb^* are the differences in L*, a*, b* coordinates between a sample and a standard.

The Neugebauer Equations for Calculations of Tristimulus Values of Three-Color Overprints [7, 8]

When printing with the three process inks; cyan, magenta, and yellow, the following eight primaries result as shown in Figure 4: white (paper), cyan, magenta, yellow, red, green, blue, and black (3-color).

In 1924, Demichel proposed the following equations for determining the relative areas of the eight primaries when the cyan, magenta, and yellow dot areas per unit area of white paper are known.

(2.9a) $$F_W = (1-c)(1-m)(1-y)$$

(2.9b) $$F_C = c(1-m)(1-y)$$

(2.9c) $$F_M = m(1-c)(1-y)$$

(2.9d) $$F_Y = y(1-c)(1-m)$$

(2.9e) $$F_R = my(1-c)$$

(2.9f) $$F_G = cy(1-m)$$

(2.9g) $$F_B = cm(1-y)$$

(2.9h) $$F_K = cmy$$

where:

F_W, F_C, F_M, F_Y, F_R, F_G, F_B, and F_K sequentially denote the fractional areas of Paper, Cyan, Magenta, Yellow, Red, Green, Blue, and Three-Color Overprint.

c denotes the fractional area covered by cyan dots.

m denotes the fractional area covered by magenta dots.

y denotes the fractional area covered by yellow dots.

cmy denotes the fractional area covered by cyan, magenta, and yellow dots, or the three-color overprint.

1-c denotes the area not covered by cyan dots.

1-m denotes the area not covered by magenta dots.

1-y denotes the area not covered by yellow dots.

(1-c)(1-m)(1-y) denotes the area not covered by cyan, magenta, and yellow dots, or white (paper).

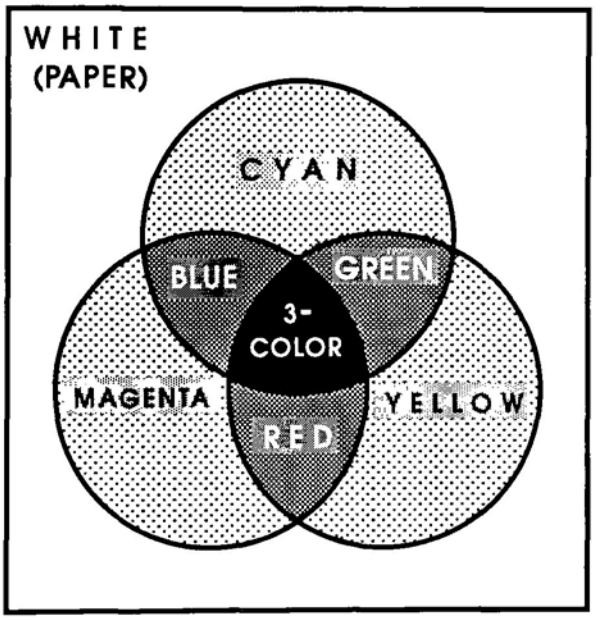

Figure 4. The Eight Primaries incorporate the Three First Primaries, Cyan, Magenta, and Yellow; the Three Secondary Primaries (Two Colored Overprints), Red, Green, and Blue; the Tertiary Primary (Three Colored Overprint); and Paper White.

Hans Neugebauer (1937) modified the Demichel's equations by taking account of the CIE tristimulus values of the eight primaries. The Neugebauer equations are based on the concept that the tristimulus values of the printed color reproduced by printing with cyan, magenta, and yellow inks can be attained by adding up the tristimulus values of the eight primaries each weighted by its fractional area. The Neugebauer equations, hence, can be shown as follows:

$$X_{PC} = F_W X_W + F_C X_C + F_M X_M + F_Y X_Y + F_R X_R + F_G X_G + F_B X_B + F_K X_K \quad (2.10a)$$

$$Y_{PC} = F_W Y_W + F_C Y_C + F_M Y_M + F_Y Y_Y + F_R Y_R + F_G Y_G + F_B Y_B + F_K Y_K \quad (2.10b)$$

$$Z_{PC} = F_W Z_W + F_C Z_C + F_M Z_M + F_Y Z_Y + F_R Z_R + F_G Z_G + F_B Z_B + F_K Z_K \quad (2.10c)$$

where X_{PC}, Y_{PC}, and Z_{PC} are the computed tristimulus values of a printed color; X_W, Y_W, Z_W,..., X_Y,Y_Y,Z_Y,..., X_K, Y_K, and Z_K are the measured tristimulus values of the eight primaries consecutively; and F_W, F_C, F_M,. . . , and F_K are the weighing fractional areas of the eight primaries.

The n-Modified Neugebauer Equations

Irving Pobboravsky, in 1965, proved that the Neugebauer equations were inaccurate to predict the tristimulus values of a neutral area. Due to optical dot gain arising from multiple internal reflections, scattering, and trapping of light within paper (the light trapped under the halftone dots causes a shadow around the dots), the Neugebauer Equations require modifying. The correction recommended in 1951 by Yule and Colt can be accomplished by using the Yule-Nielsen n-parameter in converting the

measured tristimulus values of the eight primaries into the effective tristimulus values:

(2.11a) $$X' = (X)^{1/n}$$

(2.11b) $$Y' = (Y)^{1/n}$$

(2.11c) $$Z' = (Z)^{1/n}$$

where X′,Y′, and Z′ are the effective or corrected tristimulus values of a printed color; X, Y, and Z are the measured tristimulus values of each primary; and n is the Yule-Nielsen correction factor.

The Neugebauer Equations are modified by substituting the X, Y, and Z with the X′,Y′, and Z′:

(2.12a) $$X'_{PC} = F_W X'_W + F_C X'_C + F_M X'_M + F_Y X'_Y + F_R X'_R + F_G X'_G + F_B X'_B + F_K X'_K$$

(2.12b) $$Y'_{PC} = F_W Y'_W + F_C Y'_C + F_M Y'_M + F_Y Y'_Y + F_R Y'_R + F_G Y'_G + F_B Y'_B + F_K Y'_K$$

(2.12c) $$Z'_{PC} = F_W Z'_W + F_C Z'_C + F_M Z'_M + F_Y Z'_Y + F_R Z'_R + F_G Z'_G + F_B Z'_B + F_K Z'_K$$

where:

X'_{PC},Y'_{PC}, and Z'_{PC} are the effective tristimulus values of a printed color.

X'_W, Y'_W, Z'_W, . . . , X'_Y,Y'_Y,Z'_Y, . . . , X'_K, Y'_K, and Z'_K are the effective tristimulus values of the eight primaries consecutively.

F_W, F_C, F_M, . . . , and F_K are symbolized for the fractional areas of the eight primaries consecutively.

The selection for the n-correction factor varying between 1 and 3 is predominantly dependent upon a screen ruling and a paper type. Milton Pearson, in 1980, conducted an experiment by comparing the calculated dot areas using the Yule-Neilsen equation with the actual dot areas. As a result of his experiment, Pearson concluded that the optimum n value for general conditions should be 1.7. The n value of 1.7 yields an efficacious compromise between convenience and accuracy.[9]

A New Model for Predicting the Color of Multicolor Halftone Tints[10]

Stephen Viggiano developed a new mathematical model for multicolor halftone tints by extending the Spectral Yule-Nielsen Equation, namely, modifying the "Spectral" Neugebauer Equation with the Yule-Nielsen n parameter. This new model predicts the color of multicolor halftone tints more accurately than the n-modifed Neugebauer Equations. He stated that " The non-linearities in the Spectral Yule-Nielsen model requires that narrowband measurements be used. This is because the non-linearities in the Spectral Yule-Nielsen Equation require that reflectance curve of each primary be nearly constant in each prediction band." He also suggested that "Spectrophotometric measurements, with bandwidths of 10 nm or smaller, were able to provide a significant increase in the accuracy of the color predicted for single-color halftone tints." The model for predicting the spectral reflectance of three-color halftone tints is presented as follows:

$$\text{(2.13a)} \qquad \Re_{PC}(\lambda) = [F_W \Re'_W(\lambda) + F_C \Re'_C(\lambda) + F_M \Re'_M(\lambda) + F_Y \Re'_Y(\lambda) + F_R \Re'_R(\lambda) + F_G \Re'_G(\lambda) + F_B \Re'_B(\lambda) + F_K \Re'_K(\lambda)]^n$$

(2.13b) $$\Re' = \Re^{1/n}$$

where $\Re_{PC}(\lambda)$ is the spectral reflcetance of the three-color halftone tint at the wavelength λ; $\Re'_W(\lambda)$, . . . , $\Re'_Y(\lambda)$, . . . , $\Re'_K(\lambda)$ are the effective spectral reflectances of the eight primaries at the wavelength λ; F_W , . . . , F_Y, . . . , F_K are the fractional areas weighting the reflectances of the eight primaries; and n is the selected Yule-Nielsen correction parameter.

In this study, the optimum n value of 1.7, which was suggested by Pearson, is raised to 2 for the following reasons:

(1) This research work is associated with printing at high screen frequency of 150 lines per inch; and

(2) The inaccuracy of the new model affected by a halftone dot fringe can be amended with this n value.

Endnotes for Chapter 2

[1]Miles Southworth and Donna Southworth, eds. , "Densitometry," in *Quality and Productivity in the Graphic Arts* (New York: Graphic Arts Publishing, 1989), 1-26.

[2]Commission Internationale de l' Éclairage (CIE), *Colorimetry*, Pub. No. 15.2, 2d. ed. (Vienna, Austria: Central Bureau of the CIE, 1986).

[3]American National Standards Institute, *American National Standard for Photography (Sensitometry)–Density Measurements–Spectral Conditions*, ANSI/ASC PH2.18 (New York: American National Standards Institute, 1984).

[4]Robert Chung and John Compton, "A Colorimetric Method for Visualizing and Determining Color Tolerances of Printed Colors," in *TAGA Proceedings* (Rochester, NY: Technical Association of the Graphic Arts, 1991), 120.

[5]Richard S. Hunter and Richard W. Harold, eds. , "Other Scales for Color Identification," in *The Measurement of Appearance*, 2d ed.(New York: John Wiley & Sons, 1987) , 224.

[6]Fred W. Billmeyer, Jr. and Max Saltzman, "Describing Color?," in *Principles of Color Technology*, 2d ed. (New York: John Wiley & Sons, 1981), 34-66.

[7]Gary G. Field, "Color Separation and Correction," in *Color and Its Reproduction* (Pittsburgh, PA: Graphic Arts Technical Foundation, 1988) , 224-7.

[8]Steven J. Harrington, "An Analytical Solution to the Neugebauer Equations," in *TAGA Proceedings* (Rochester, NY: Technical Association of the Graphic Arts, 1991), 144-53.

[9]Milton Pearson, "n Value for General Conditions," in *TAGA Proceedings* (Rochester, NY: Technical Association of the Graphic Arts, 1980), 415-25.

[10]J. A. Stephen Viggiano, "Modeling the Color of Multi-Colored Halftones," in *TAGA Proceedings* (Rochester, NY: Technical Association of the Graphic Arts, 1990), 44-62.

Chapter 3

A Review of the Literature in the Field

This research is meant to relate the densitometric SID and dot gain tolerances standardized by FIPP to the colorimetric tolerances. No references to this research work were found where this problem was investigated. Therefore, this literature review covers only the topics related to the broad aspects of dot gain, color variation, the CIE system, and the Neugebauer Equations. The explored research works are described as follows:

In 1984, Jang-fun Chen[1] presented his research work, An investigation of color variation as a function of register in dot-on-dot multicolor printing, at the 36th Annual TAGA Conference. He developed a mathematical model and employed the Neugebauer equations modified with nine n values for all tristimulus values for quantifying color variations due to misregister of each of three process inks (cyan, magenta, and yellow) at three dot area levels of 25%, 50%, and 75%. The proposed mathematical model was proved to be successful for predicting the CIE ΔE^*_{ab} of the misregistered colors and indicating the latitudes of dot misplacement that produced color variations.

In 1986, Dawn Leslie Link[2] investigated the effects of screen rulings and dot structures on dot gain in offset newsprint. The square, round, and elliptical dot structures and four screen rulings of 65, 85, 100, and 150 lines per inch were the chosen variables to be tested on how each of them influences dot gain. It was found that a coarse screen ruling yielded less dot gain than a fine screen ruling and that there was no significant difference in the amount of dot gain among the three different dot structures.

In 1988, Patchanee Malikhao and Mary Louise Bulger conducted analogous research works. Malikhao[3] varied the printing sequences of four process inks to study wet trapping efficiency and color variation in web-offset printing. The different printing ink sequences yielded different color gamuts in the CIELAB color space. She also concluded that the most appropriate printing sequence was YMCK because it produced the highest trapping percentages and provided the least total color differences from the ideal inks. Bulger[4] utilized the IGT printability tester in simulating ink trapping and analyzed color variations due to changes in ink trapping by colorimetric means. The trapping conditions were simulated by varying film thickness levels of the SWOP process inks. As a result of her experiment, the changes in gravimetric trapping percentages caused changes in the CIE L^*_{ab}, C^*_{ab}, and h°_{ab} values; which means that there was a change in the overall color appearance.

In 1989, Amal A. Ba'adarani[5] studied the magnitude of doubling at different angles in the offset printing process. Concentric circles, which are the main element of the RIT doubling test target, were inspected for the occurrence of doubling in her work. It was shown that there was a relationship between doubling magnitude and doubling angle.

In 1990, J. A. Stephen Viggiano[6] extended the Spectral Yule-Nielsen model developed for predicting color of single-colored halftone tints to a new mathematical model for multicolor halftone tints. The accuracy of the new model in predicting color of multicolor halftone tints is achieved by applying narrowband measurements. The new model has greater accuracy in predicting color of multicolor halftone patterns than the n-modified Neugebauer Equations. The experimental geometric mean of the CIE ΔE^*ab values between measured values and predicted values was merely 1.82. This assures that the new model predicts color of halftone tints very accurately.

In 1991, James B. Mudge[7] explored the effect of the varied printing speeds of a lithographic press on dot gain. The press was operated at 600 fpm, 800 fpm, 1000 fpm, and 1200 fpm. The results of the experiment indicated that there was an inverse relationship between press speed and dot gain, i.e., as the press speed increased, the amount of dot gain decreased.

In the same year, Kuang-Hua Sun[8] studied the relationship between dot gain and dot shape and the validity of border zone theory in explaining the happening of mechanical dot gain among four different halftone dot shapes; one square dot, two round dots, and one diamond-shaped dot. The final result of his study did not support the border zone theory and the location of the highest amount of dot gain was affected by dot shape and corner-linkup phenomenon.

This study will mainly depend on a mathematical model that can predict the CIELAB values of a color produced by a mixture of three-color halftone tints. The accuracy of the experimental results is therefore based on the accuracy of the mathematical model in predicting color of halftone

tints. As stated earlier, the extended Spectral Yule-Nielsen model developed by Stephen Viggiano yields accurate predictions of the color of halftone tints. In order to complete this study, this new model will be the prime model to be employed.

Most of the research works reviewed in this chapter were attempts to study some independent variables that bring forth dot gain and color variations. Although they are not directly relevant to this study, they provide useful basic knowledges of dot gain and color variation that are supportive of this study.

Endnotes for Chapter 3

[1]Jang-fun Chen, "An Investigation of Color Variation As a Function of Register in Dot-on-Dot Multicolor Halftone Printing," in *TAGA Proceedings* (Rochester, NY: Technical Association of the Graphic Arts, 1984), 315-33.

[2]Dawn Leslie Link, "An Investigation of the Effects of Screen Ruling and Dot Structure Have on Dot Gain on Offset Newsprint" (M.S. thesis, Rochester Institute of Technology, 1986).

[3]Patchanee Malikhao, " The Application of CIELAB to Study Trapping Efficiency" (M.S. thesis, Rochester Institute of Technology, 1988).

[4]Mary Louise Bulger, " A Colorimetric Analysis of Color Variation Due to Changes in Simulated Ink Trapping" (M.S. thesis, Rochester Institute of Technology, 1988).

[5]Amal A. Ba'adarani, "A Study on Doubling in the Offset Printing Process" (M.S. thesis, Rochester Institute of Technology, 1989).

[6]J. A. Stephen Viggiano, " Modeling the Color of Multi-Colored Halftones," in *TAGA Proceedings* (Rochester, NY: Technical Association of the Graphic Arts, 1990), 44-62.

[7]James B. Mudge, "A Study of the Effect of Lithographic Press Speed on Dot Gain" (M.S. thesis, Rochester Institute of Technology, 1991).

[8]Kuang-Hua Sun, "A Study of Mechanical Dot Gain for Different Dot Shapes Based on the Border Zone Theory" (M.S. thesis, Rochester Institute of Technology, 1991).

Chapter 4

The Hypotheses

Statement of the Hypothesis

Based on the objectives, theories, and relevant research works, mentioned in the preceding chapters, the hypotheses for this research are formulated as follows:

(1) *Neutrality of Aim Gray*:

The CIE Chroma of an overprint of 75% cyan dot area, 62% magenta dot area, and 60% yellow dot area, printed to the FIPP specifications for printing at 150 line screen on coated paper and with positive-working plate is less than the just noticeable Chroma difference of 2 ΔC^*_{ab} units.

(2) *Maximum CIELAB Deviation from Aim*:

The largest CIE ΔE^*_{ab} values between the gray produced by printing to the FIPP aim values of solid ink densities and dot gain and all the other near grays produced by the FIPP tolerances for solid ink densities and dot gain are less than 6 ΔE^*_{ab} units.[1]

(3) *Uniformity of Deviations from Aim*:

All the ΔE^*_{ab} values between the aim gray and the near grays are the same within 2 ΔE^*_{ab} units.

(4) *Equivalence of Traditional and Colorimetric Tolerances*:

The ellipsoidal CIELAB tolerances can be defined so that they are equivalent (within 2 units of the CIE ΔE^*_{ab}) to tolerances based on specifications of solid ink density tolerances and dot gain tolerances.

Endnote for Chapter 4

[1]Scott Stamm, "A Colorimetric Investigation of Color Tolerances" (M.S. thesis, Rochester Institute of Technology, 1980).

Chapter 5

Methodology

Delimitation of the Study

The purpose of this investigation is to mathematically convert the densitometric dot gain and SID tolerance specifications into the colorimetric tolerances. These tolerances will be set forth for high quality printing on coated stock, at a 150 line screen, with a positive-working plate. This specific printing condition is used as a criterion for designating which SID and dot gain specifications are going to be conformed to in this study. After comparing several printing standards, the FIPP specifications for SID and dot gain are selected as standard for the following reasons:

(1) The SWOP specifications are intended for web-offset printing at only a screen ruling of 133 lines per inch with a negative-working plate. This SWOP specified printing condition is significantly different from the aimed printing condition. In the US, the specifications for commercial printing have not yet been defined.

(2) FOGRA provides no actual SID aim values but specifies only percent SID tolerance instead. To attain the actual density values, secondary color standards have to be produced on production paper in a

manner that their ink film thicknesses (IFTs) match the ones of the FOGRA primary color standards. The production of the secondary color standards according to the FOGRA procedures are complicated; hence, its specifications are not used.

(3) FIPP provides the SID aim value and tolerances for density readings with broad-band, narrow-band, and polarized filters and the dot gain tolerances for both positive- and negative- working plates at five dot area percentages. It is evident that the FIPP specifications for SID and dot gain are the most comprehensive and useful.

Formulation of Null and Alternative Hypotheses[1]

Before the experimental data can be statistically interpreted, the null and alternative hypotheses need to be clearly stated. The statistical technique of two-way analysis of variance is the principal tool for testing the hypotheses since the experiment of this study simultaneously involves two factors; changes of C-M-Y dot area combinations and of C-M-Y SID combinations. To draw inferences about the means from the data of the CIELAB coordinates and the CIE color differences, the null and alternative hypotheses are formulated as follows:

$$H_{01}: \alpha_1 = \alpha_2 = \alpha_3 = \ldots = \alpha_{15}$$

$$H_{02}: \beta_1 = \beta_2 = \beta_3 = \ldots = \beta_{15}$$

$$H_A: \text{at least one inequality exists}$$

where:

$\alpha_i = \mu_{i.} - \mu_{..}$; i = 1, 2, 3, . . . , 15 (the difference between the means of the data, $\mu_{i.}$, due to change of C-M-Y SID combinations and the mean of the overall data, $\mu_{..}$)

$\beta_j = \mu_{.j} - \mu_{..}$; j = 1, 2, 3, . . . , 15 (the difference between the means of the data, $\mu_{.j}$, due to change of C-M-Y dot area combinations and the mean of the overall data, $\mu_{..}$)

Experimental Design

Both Gretag and FOGRA recommend using the following dot areas on film to produce a dark neutral gray: 75% cyan dot area, 62% magenta dot area, and 60% yellow dot area. This dot area combination was selected and used as the reference dark gray for this investigation.

Referring to the FIPP dot gain tolerances for printing on coated supercalendered paper with a positive-working plate, the apparent dot area specifications for cyan, magenta, and yellow are 75% + (14% $\pm$ 2%), 62% + (17% $\pm$ 2%), and 60% + (18% $\pm$ 2%), respectively. Because FIPP has specified that the amount of dot gain in each process ink should be uniformly high or low, the 15 acceptable combinations of cyan, magenta, and yellow apparent dot areas are obtained by subtracting the 12 unacceptable combinations from the total 27 possible combinations (See Figure 4).

The reasons why the FIPP specifications for narrowband, nonpolarized densitometry were used for this study are:

(1) The narrowband densitometer, rather than the wideband densitometer, has been used for process control on account of the

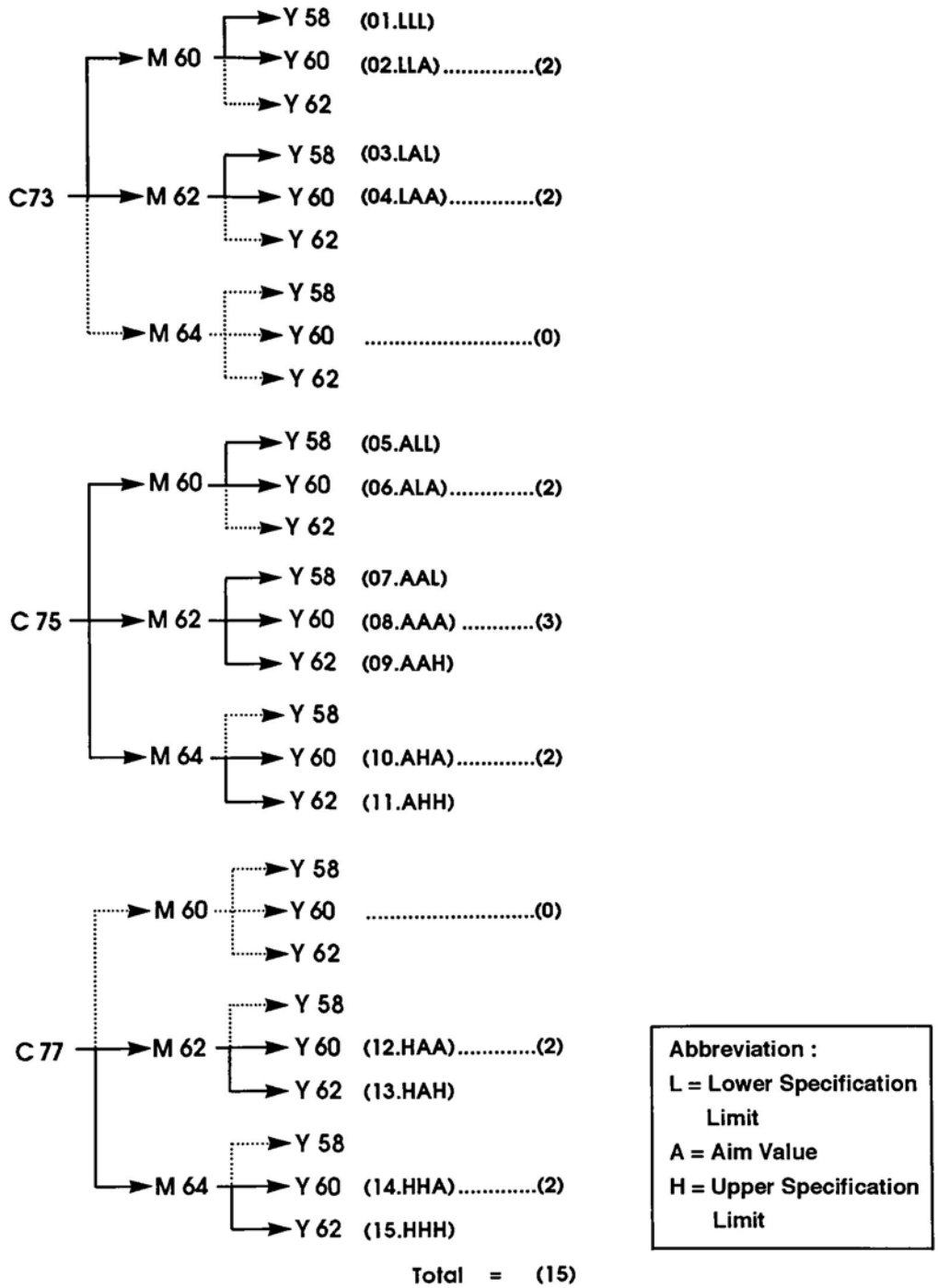

Figure 4. Tree diagram portrays the 15 C-M-Y film dot area combinations in conformance with the FIPP dot gain tolerance window; a dotted arrow designates a combination that falls out of the FIPP dot gain specifications.

insensitivities of wideband filters to IFT variations, especially to yellow IFT; and

(2) The computer programs were developed by not taking the effect of polarizing filter into account.

The FIPP tolerance window for SID read through a narrow-band, nonpolarized filter when printing on a coated supercalendered woodfree paper fall within the range of -0.0 to + 0.2. The deviations of solid ink densities also have to be uniformly high or low. Thus only 15 combinations out of the total 27 possible combinations are allowed (See Figure 5). As a result, the total combinations of cyan, magenta, and yellow apparent dot areas for 15 different combinations of solid ink densities are equivalent to 225 (or 15x15).

In theory, one could print all 225 possible combinations, take measurements and then arrive at the predicted colorimetric tolerances. In practice, this is humanly impossible because a press could not be expected to produce the precise demanded results in any printing unit. The only practical solution to this problem is therefore by using the computer program that can predict the colorimetric values of three-color overprint halftone grays at the simulated printing conditions of interest.

Functions of the Computer Programs [2]

The following is a description of the three computer programs that were utilized to perform the calculations. These programs were written by Mr. J.A. Stephen Viggiano, Senior Imaging Scientist, RIT Research Corporation:

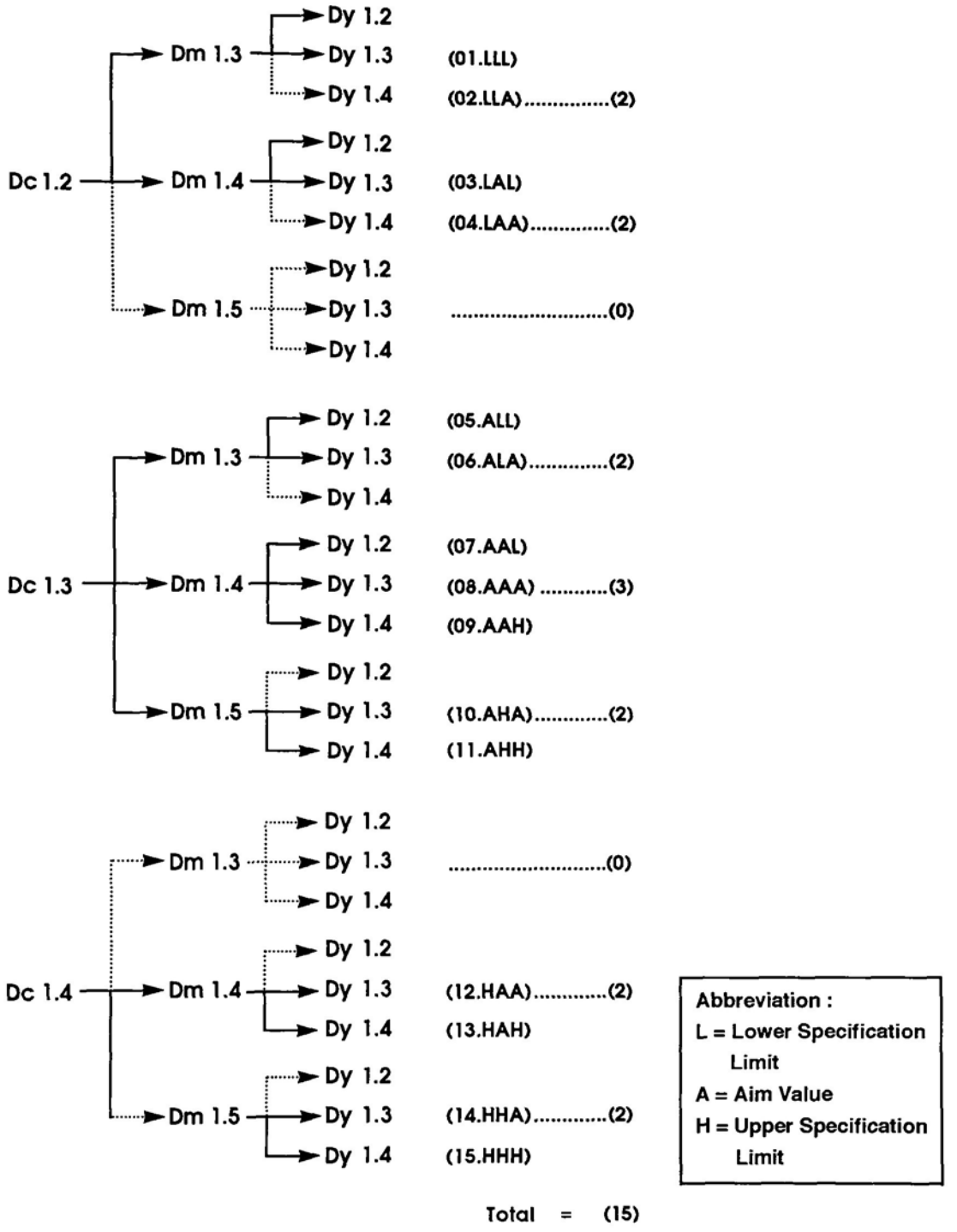

Figure 5. Tree diagram depicts all the 15 SID combinations of Cyan, Magenta and Yellow conforming to the FIPP SID specifications; a dotted arrow indicates a combination that falls out of the FIPP SID specifications.

1. The Change Solid Ink Density (CSID) Program is composed of executable and default files. The executable one, CSID.EXE, is based on the GRL Trapping model that carries on the task of predicting the new spectral reflectances of the eight primaries when a change of cyan, magenta, or yellow SID level takes place. The spectral reflectances are then converted into the spectral densities and the CIELAB coordinates. The default file, CSID.DEF, contains the input data that are essential for the CSID.EXE file. These data are sequentially listed below:

(a) The wavelength range of 380nm to 720nm with 10nm increment interval;

(b) The Yule-Nielsen n-value of 2.00;

(c) The name of a file containing the spectral weighting functions for the CIE Illuminant D_{50} and the CIE 1964 Supplementary Standard Observer (10°); and

(d) The name of a file containing the spectral products of the Status E (narrowband) densitometry.

2. The Solid Ink Density Check (SIDCHECK) Program does a verification of the outputs from executing the CSID program.

3. The Viggiano Model (VMODEL) Program calculates the CIELAB coordinates of the three-color overprint halftone grays. The colorimetric results are achieved by the Yule-Nielsen modified Spectral Neugebauer model that is incorporated in the VMODEL.EXE program. The input file of 15 FIPP C-M-Y dot area combinations is required as a source that is later used by the program for generating the Demichel fractional dot areas. The

contents of the VMODEL.DEF file are similar to the CSID.DEF file, except that the mechanical dot gain figures at 50% dot area of the process inks and the name of a file containing the spectral reflectance factors of the eight Neugebauer Primaries are additionally included with the file.

The VMODEL program requires entering the mechanical dot gain figure at 50% dot area pertaining to the Yule-Nielsen n-value of 2. The optical effect of the FIPP allowable apparent dot gain (a combination of optical and mechanical dot gain), hence, must be excluded. The procedure to achieve this dot gain figure will be expounded in detail in the section below.

Experimental Procedures

(1) The file of the reference (aim) spectral reflectances of the eight Neugebauer Primaries [3] (See Table A3 in Appendix A), which are the CEI30–89 Standardized Inks printed to the FIPP aim SID levels, was created as a text file. The name of this text file was entered while the CSID.EXE program was executed. The program then computed the spectral (aim) densities of cyan, magenta, and yellow inks and their correspondent CIELAB coordinates.

(2) The SID of cyan, magenta, or yellow ink was changed by ± 0.10 off the computed aim values from (1) in conformance with the FIPP SID tolerance specifications (See Figure 5) for each of the 14 runs of the CSID.EXE program. The 14 output Primaries files containing the new spectral reflectances of the eight Neugebauer Primaries and their new CIELAB coordinates were then produced.

(3) The total 15 output Neugebauer Primaries files from executing the CSID program were verified by loading these files to the SIDCHECK program. These output files were the input files for the VMODEL.EXE program.

(4) The text file of the 15 FIPP C-M-Y dot area combinations (Demichel fractional dot areas) illustrated in Figure 4 was generated. These dot areas were typed as decimal fractions.

(5) The Yule-Nielsen (excluding optical dot gain) dot gain figures of cyan, magenta, and yellow inks, which are equal to 2.05%, 0.84%, and 3.64%, respectively, were entered as decimal fractions into the VMODEL.DEF file by utilizing a text editor program. The calculations of dot gain figures at 50% dot area from the Yule-Nielsen dot areas on paper are demonstrated in Appendix B.

(6) The text file of the 15 FIPP C-M-Y dot area combinations was loaded to the VMODEL.EXE program. By operating the VMODEL.EXE program the CIELAB coordinates and the Status E densities of three-color overprint grays at 15 different FIPP C-M-Y dot area combinations were predicted. As a result of executing the VMODEL.EXE program fifteen times (15 files of the Neugebauer Primaries), the CIELAB coordinates of 225 three-color overprint gray were obtained.

(7) The CIELAB coordinates of the overall 225 grays were then graphically displayed and statistically analyzed by the JMP program.[4]

(8) The color difference (ΔE^*_{ab}) values between the aim gray and the other 224 grays were calculated by the EXCEL spreadsheet program, whereas the MINITAB program was employed to perform TWOWAY ANOVA on each set of L*, a*, b*, and ΔE^*_{ab} data.

Figure 7 illustrates an algorithm of the experimental procedures in predicting the CIELAB coordinates of the 225 three-color overprint halftone grays.

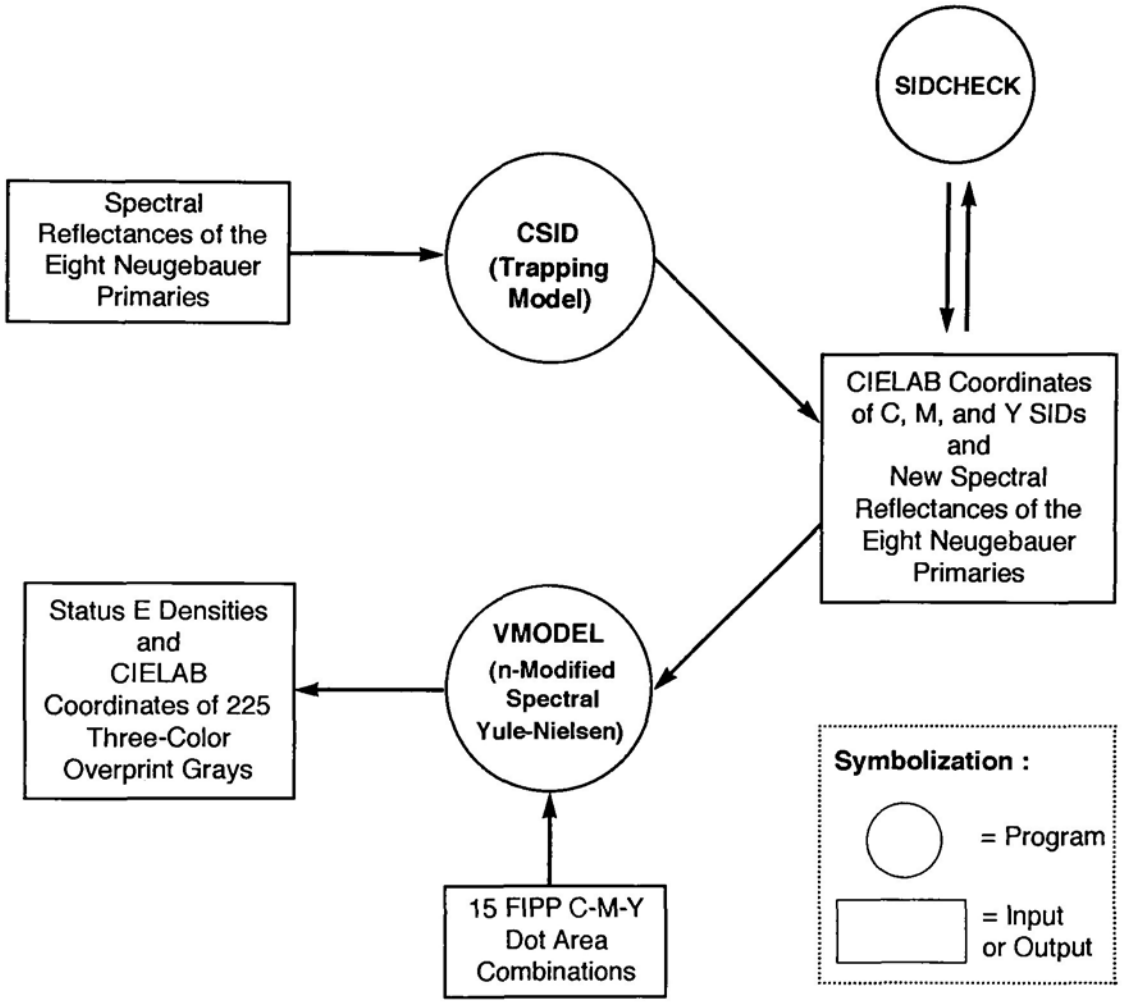

Figure 7. Algorithms in predicting the CIELAB coordinates of 225 three-color overprint halftone grays

Endnotes for Chapter 5

[1]Shirley Dowdy and Stanley Wearden, *Statistics for Research*, 2d. ed. (New York:John Wiley & Sons, 1991).

[2]J. A. Stephen Viggiano, *Personal Communication*, 1992.

[3]EMPA/UGRA, *The Spectral Reflectance Values for Ink Colors and Paper for Multi-Color Printing*, CEI 30–89 (St.Gallen, Switzerland: EMPA/UGRA, Dec 1992), Fax Transmission.

[4]JMP Ver. 2.0 (Cary, NC: SAS Institute).

Chapter 6

The Results

Results and Discussion

Table C1 in Appendix C contains the predicted CIELAB coordinates of the overall 225 three-color overprint halftone grays, including the calculated color difference (ΔE^*_{ab}) figures. Within the same Appendix, the correspondent Status E densities, D_r, D_g, and D_b, of these grays are also provided in Table C2 for reference and comparison, while the CIELAB coordinates of cyan, magenta, and yellow SIDs in each of the C-M-Y SID combinations are listed in Table C3.

Initially, it should be stated that Status E SIDs of cyan and yellow inks attained from computer programs do not match the FIPP aim SIDs for narrowband, nonpolarized densitometry. Status E SID of cyan ink is 0.1 higher than the aim while Status E SID of yellow ink is 0.1 lower than the aim. The possible cause for the deviation could be that FIPP and this study applied different filters with different bandwidths. Densities in this study were based on the Status E responses (47B filter with 40nm bandwidth), whereas FIPP used a SPI densitometer (SPI filters with 20nm bandwidth), e.g. Macbeth 918, for density readings. Since this study is only concerned with relative values, not absolute values, the results should still be valid.

Descriptions of the Colorimetric Specifications and Neutrality of the Grays

As a result of the mathematical conversions, the new specifications, in colorimetric units, are made up of the colorimetric elements as summarized in Table 4. The aim gray, which is an overprint of 75% cyan, 62% magenta, and 60% yellow, has the following CIELAB coordinate; 38.41 in the L* scale, -1.08 in the a* scale, and -7.89 in the b* scale. The lightness of the aim gray decreases whenever dot area (dot gain) or SID (IFT) of any ink is raised. The a* data range from negative to positive numbers without any one being zero, whereas the b* data all are negative figures. Under the D_{50} illumination and with the CIE 10° observer, the overall 225 grays therefore have a cast of either greenish blue or reddish blue. An exact neutral dark gray would have a* and b* values of zero.

Table 4.

Ranges, means, and standard deviations of the L*, a*, b*, C^*_{ab}, and ΔE^*_{ab} data of the 225 three-color overprint grays

	Range	Mean	Stdev.
L*	34.74 to 41.88	38.35	1.57
a*	-4.88 to 3.17	-0.78	1.64
b*	-11.18 to -4.67	-7.92	1.42
C^*_{ab}	4.67 to 11.33	8.12	1.43
ΔE^*_{ab}	0.25 to 4.74	2.54	0.90

Distributions of and Variations in the Predicted Colorimetric Data

To examine the distributions of the L*, a*, and b* data, the JMP program was utilized to create the histograms and the boxplots of each data set as individually illustrated in Figures 8a-8c. They prove that the L*, a*, and b* data all are normally distributed.

The standard devations of the L*, a*, b*, and C^*_{ab} data are quite similar. This is an indication that none of the dimensions (L*, a*, or b*) contribute more to color variation of the aim gray than any other one.

Colorimetric Deviations Due to Varying Dot Areas and Changing SID Levels

Tables 5 and 6 shows the colorimetric deviations ΔL*, Δa*, and Δb* figures due to varying dot areas by ± 2% and due to changing SID levels ± 0.1, respectively.

The greatest deviations in the L* and a* dimensions of the aim gray are apt to result from a change of cyan dot area or SID. Increment and decrement in the same cyan, magenta, and/or yellow dot areas exhibit approximately symmetrical changes in the L*, a*, and b* values as shown in Table 5. It is likewise evident that there exists the feature of additivity among the data; for instance, the ΔL* value of simultaneously increasing in 2% dot areas of both cyan and magenta inks (=-1.42) can be estimated by adding up the individual ΔL* values of increasing in 2% dot area of cyan (=-0.69) and magenta inks (=-0.74) and so forth. However, for changes in SID levels, there exist no such symmetry and additivity.

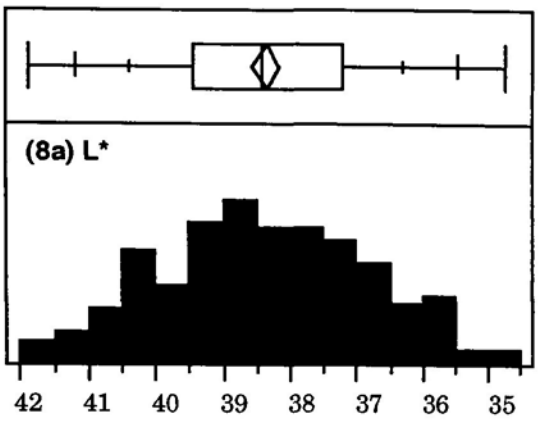

Statistical Analysis on **L*** by JMP

Max	41.8800
Min	34.7400
Median	38.4100
Mean	38.3508
Std Dev	1.5737
Std Err Mean	0.1049
Upper 95% Mean	38.5575
Lower 95% Mean	38.1440
N	225.0000
Sum Wgts	225.0000

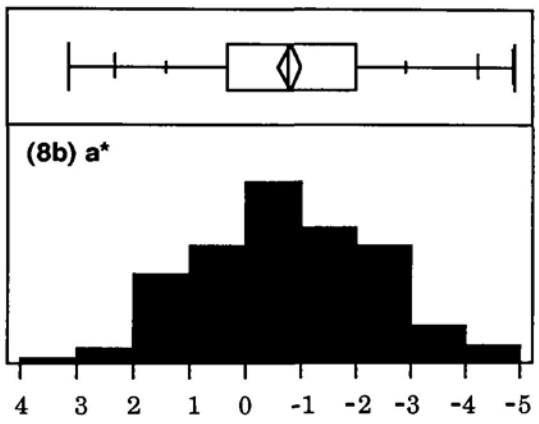

Statistical Analysis on **a*** by JMP

Max	3.1700
Min	-4.8800
Median	-0.7600
Mean	-0.7830
Std Dev	1.6392
Std Err Mean	0.1093
Upper 95% Mean	-0.5676
Lower 95% Mean	-0.9983
N	225.0000
Sum Wgts	225.0000

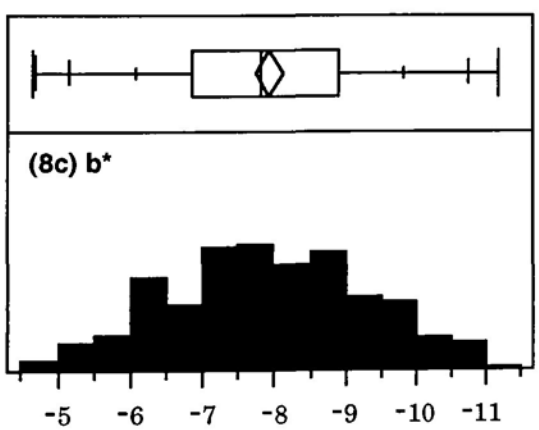

Statistical Analysis on **b*** by JMP

Max	-4.6700
Min	-11.1800
Median	-7.8100
Mean	-7.9220
Std Dev	1.4158
Std Err Mean	0.0944
Upper 95% Mean	-7.7360
Lower 95% Mean	-8.1080
N	225.0000
Sum Wgts	225.0000

Figure 8. Histograms, boxplots and statistical analyses manifest the distributions and characteristics of the individual L* (8a), a* (8b), and b* (8c) data.

Table 5. Ranges, means, and standard deviations of the ΔL*, Δa*, and Δb* data due to varying cyan, magenta, and/or yellow dot areas by ± 2% off the aim value

Change in Dot Areas of C, M, and/or Y	ΔL*			Δa*			Δb*		
	Range	Mean	Stdev.	Range	Mean	Stdev.	Range	Mean	Stdev.
-2% DAs of C, M, & Y	1.48 to 1.56	1.52	0.03	0.13 to 0.42	0.28	0.08	0.11 to 0.23	0.17	0.04
-2% DAs of C & M	1.40 to 1.48	1.44	0.02	-0.10 to 0.13	0.01	0.06	1.43 to 1.49	1.46	0.02
-2% DAs of C &Y	0.74 to 0.81	0.77	0.02	1.81 to 1.99	1.92	0.06	-0.27 to -0.13	-0.20	0.04
-2% DA of M &Y	0.79 to 0.85	0.81	0.02	-1.44 to -1.26	-1.35	0.06	-0.97 to -0.85	-0.91	0.04
-2% DAs of C	0.67 to 0.74	0.70	0.02	1.57 to 1.72	1.65	0.05	1.05 to 1.12	1.08	0.02
-2% DA of M	0.71 to 0.78	0.74	0.02	-1.73 to -1.56	-1.63	0.05	0.36 to 0.40	0.38	0.01
-2% DA of Y	0.06 to 0.08	0.08	0.01	0.24 to 0.31	0.28	0.02	-1.35 to -1.22	-1.28	0.04
+2% DA of Y	-0.08 to -0.06	-0.07	0.01	-0.30 to -0.23	-0.27	0.02	1.22 to 1.35	1.28	0.04
+2% DA of M	-0.77 to -0.71	-0.74	0.02	1.56 to 1.75	1.65	0.05	-0.39 to -0.35	-0.38	0.01
+2% DA of C	-0.72 to -0.66	-0.69	0.02	-1.74 to -1.60	-1.67	0.05	-1.11 to -1.04	-1.07	0.02
+2% DA of M & Y	-0.84 to -0.78	-0.81	0.02	1.27 to 1.49	1.38	0.06	0.84 to 0.94	0.89	0.03
+2% DAs of C &Y	-0.80 to -0.73	-0.77	0.02	-2.04 to -1.84	-1.96	0.06	0.13 to 0.27	0.20	0.04
+2% DAs of C &M	-1.46 to -1.38	-1.42	0.02	-0.16 to 0.08	-0.04	0.07	-1.48 to -1.40	-1.44	0.02
+2% DAs of C, M, & Y	-1.54 to -1.45	-1.50	0.02	-0.46 to -0.16	-0.32	0.08	-0.25 to -0.13	-0.18	0.04

Table 6. Ranges, means, and standard deviations of the ΔL*, Δa*, and Δb* due to varying cyan, magenta, and/or yellow SIDs by ± 0.1 off the aim

Change in SIDs of C, M, and/or Y	ΔL*			Δa*			Δb*		
	Range	Mean	Stdev.	Range	Mean	Stdev.	Range	Mean	Stdev.
–0.1 SIDs of C, M, & Y	1.95 to 2.04	1.99	0.03	0.32 to 0.57	0.44	0.08	-0.74 to -0.21	-0.70	0.03
–0.1 SIDs of C & M	1.70 to 1.79	1.74	0.03	0.46 to 0.74	0.59	0.06	1.10 to 1.22	1.16	0.04
–0.1 SIDs of C & Y	1.14 to 1.20	1.17	0.02	1.57 to 1.82	1.69	0.08	-0.71 to -0.59	-0.65	0.04
–0.1 SIDs of M & Y	0.92 to 0.99	0.96	0.02	-1.35 to -1.06	-1.20	0.09	-1.71 to -1.63	-1.67	0.03
–0.1 SID of C	0.92 to 0.96	0.94	0.01	2.29 to 2.61	2.44	0.10	0.84 to 0.87	0.85	0.01
–0.1 SID of M	0.82 to 0.88	0.85	0.02	-1.87 to -1.69	-1.78	0.05	0.20 to 0.28	0.24	0.03
–0.1 SID of Y	0.03 to 0.04	0.03	0.01	0.08 to 0.25	0.17	0.05	-1.93 to -1.80	-1.87	0.04
+0.1 SID of Y	-0.41 to -0.38	-0.39	0.01	-0.42 to -0.23	-0.32	0.06	1.47 to 1.60	1.53	0.05
+0.1 SID of M	-0.82 to -0.76	-0.79	0.01	1.03 to 1.18	1.10	0.05	0.27 to 0.33	0.30	0.02
+0.1 SID of C	-1.12 to -1.04	-1.08	0.02	-0.17 to -0.03	-0.10	0.04	-1.43 to -1.28	-1.35	0.04
+0.1 SIDs of M & Y	-1.11 to -1.08	-1.09	0.02	1.09 to 1.18	1.13	0.03	1.71 to 1.83	1.77	0.04
+0.1 SIDs of C & Y	-1.32 to -1.25	-1.29	0.02	-1.28 to -0.99	-1.13	0.10	0.44 to 0.56	0.50	0.03
+0.1 SIDs of C & M	-1.92 to -1.85	-1.89	0.02	0.87 to 0.92	0.89	0.01	-1.08 to -0.94	-1.01	0.04
+0.1 SIDs of C, M, & Y	-2.17 to -2.10	-2.14	0.02	0.54 to 0.62	0.58	0.08	0.35 to 0.41	0.38	0.02

In order to find out why additivity and symmetry fail to hold for changes of SIDs, the measured and predicted spectral reflectance values of the eight primaries were reinvestigated. It was found that the spectral reflectances of red, green, blue, and 3-color overprint for the aim SID levels were obtained from actual measurements, whereas the spectral reflectances of red, green, blue, and 3-color overprints for low and high SIDs were computed from the measured cyan, magenta, and yellow spectral reflectances for the aim SIDs. Because the calculated spectral reflectance data of red, green, blue, and 3-color overprints for low and high SIDs are not exactly proportinal to the measured spectral reflectance data of red, green, blue, and 3-color overprint for the aim SIDs. A small deviation results. This probably is the reason for the additivity and symmetry failures among the ΔL^*, Δa^*, and Δb^* data due to varying SIDs.

The average numbers of the ΔL^*, Δa^*, and Δb^* data from Tables 5 and 6 are graphically compared to each other in Figures 9–11.

Since any change of cyan, magenta, and/or yellow dot areas and/or SIDs simultaneously affect both of the a* and b* dimensions, a very complex relationship results. Therefore, it could be helpful to derive the equations describing the relationships among the colorimetric data, dot areas, and SIDs.

By a multiple regression analysis performed by the JMP program with the second degree polynomial fitting, the model that can estimate the values of L*, a*, and b* from cyan, magenta, and yellow dot areas and cyan, magenta, and yellow SIDs was derived. Since the data of L*, a*, and b* are independent, but related, to each other, the three models were employed to serve the estimations of the individual colorimetric values:

(6.1a) $$L^* = -56.6167(DAf_c) + 14.5486(DAf_c)^2 - 47.6674(DAf_m) + 8.7153(DAf_m)^2 - 5.6604\,(DAf_y) + 1.6319(DAf_y)^2 - 7.122\,(SID_c) - 1.0403(SID_c)^2 - 18.8476(SID_m) + 3.7284\,(SID_m)^2 + 12.9199(SID_y) - 6.0892\,(SID_y)^2 + 126.9453$$; [$R^2 = 0.9991$ and Root MSe = 0.0491]

(6.1b) $$a^* = 3.4375(DAf_c) - 57.7083(DAf_c)^2 + 68.175(DAf_m) + 11.0417(DAf_m)^2 - 8.0333\,(DAf_y) - 4.7917(DAf_y)^2 - 238.9467(SID_c) + 77.7673(SID_c)^2 + 52.2951(SID_m) - 13.2899\,(SID_m)^2 + 56.2185(SID_y) - 23.4701\,(SID_y)^2 + 90.7124$$; [$R^2 = 0.9795$ and Root MSe = 0.241]

(6.1c) $$b^* = -67.6(DAf_c) + 9.2014(DAf_c)^2 - 6.4743(DAf_m) - 9.9653(DAf_m)^2 + 88.7271(DAf_y) - 20.7986(DAf_y)^2 + 31.4428(SID_c) - 14.6415(SID_c)^2 - 51.6114(SID_m) + 18.0716\,(SID_m)^2 + 44.611(SID_y) - 11.1884\,(SID_y)^2 - 16.2598$$; [$R^2 = 0.9951$ and Root MSe = 0.1016]

where DAf_c, DAf_m, and DAf_y denote percent cyan dot area on film, percent magenta dot area on film, and percent yellow dot area on film, respectively, and SID_c, SID_m, and SID_y denote cyan SID, magenta SID, and yellow SID, respectively.

Because all of the R^2 and root mean square error values for the three above-expressed quadratic models are very close to one and zero, respectively, they substantiate that the data are very well fitted with the models.

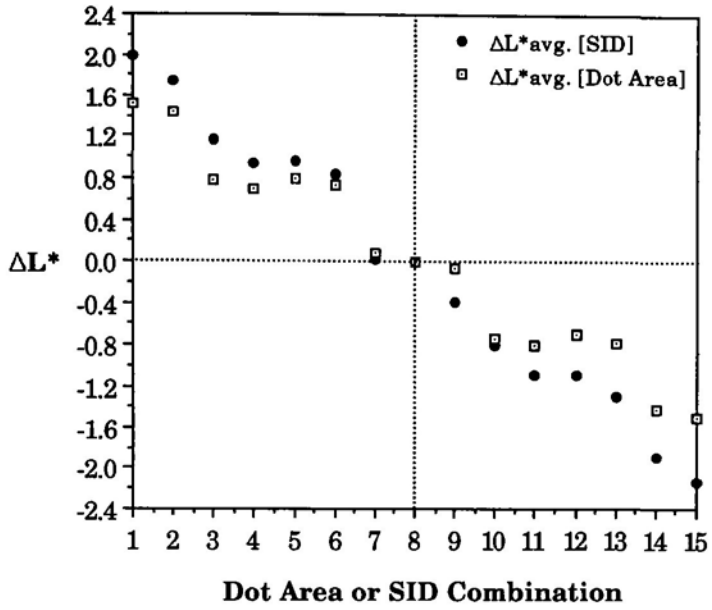

Figure 9. Comparisons among the average ΔL* data of the grays of the 15 different C-M-Y dot area combinations and the grays of the 15 different C-M-Y SID combinations.

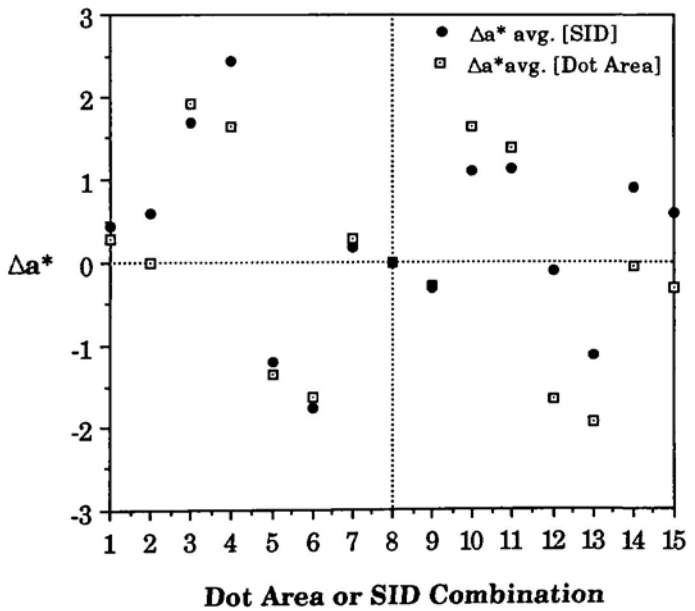

Figure 10. Comparisons among the average Δa* data of the gray of the 15 different C-M-Y dot area combinations and the grays of the 15 different C-M-Y SID combinations.

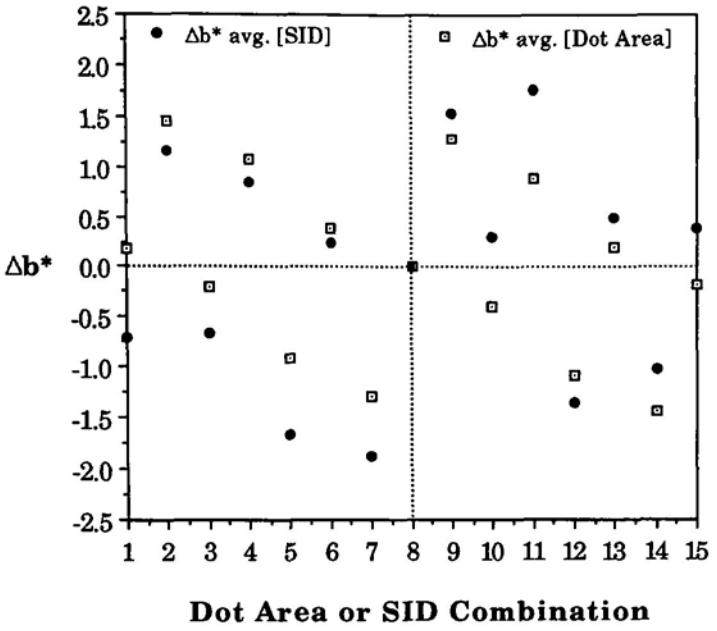

Figure 11. Comparisons among the average Δb* data of the grays of the 15 different C-M-Y dot area combinations and the grays of the 15 different C-M-Y SID combinations.

Shape of the Cluster of the Colorimetric Data Points in the L a* b* Space and Variations of Its Magnitude*

The CIELAB coordinates of the 225 grays (See Appendix C), which were located in the three-dimensional L* a* b* space by the JMP program, are illustrated in Figure 12. A cube that surrounds the axes of ΔL*, Δa*, and Δb* helps enhance the depth of the plots. The origin of the three axes is the average of the L*, a*, and b* data.

Since the CIELAB coordinate of the aim gray (L* of 38.41,a* of -1.08, and b* of -7.89) deviates slightly from the origin of the three axes, this could imply that: (1) the aim gray in densitometric units is different from the aim

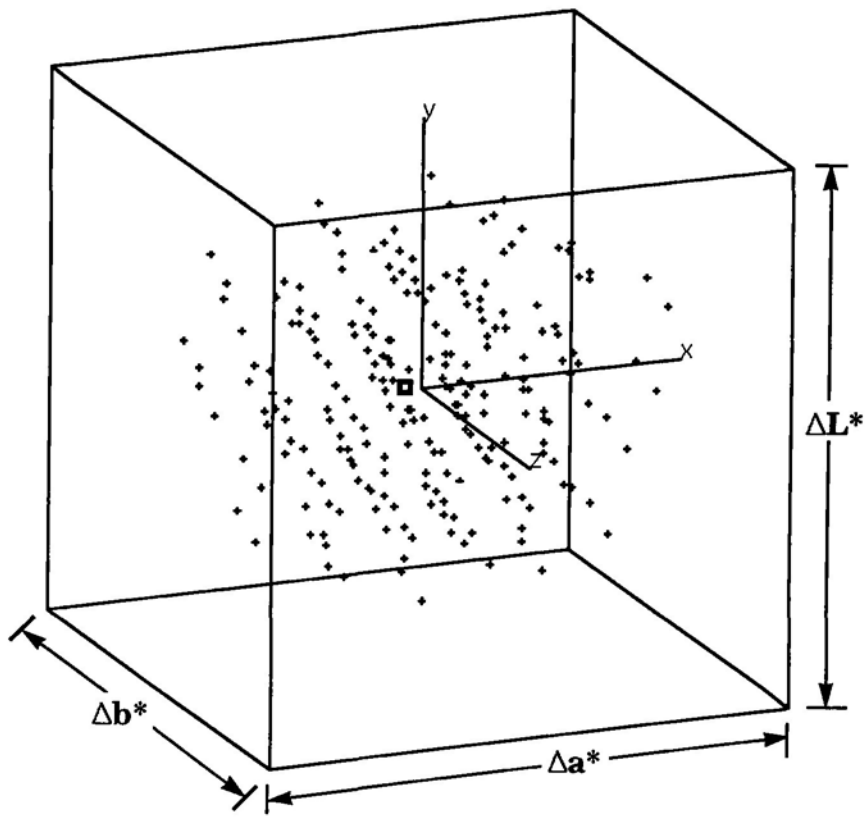

The coordinate of the origin of the three axes is L* of 38.35, a* of –0.78, and b* of –7.92 that are the averages of each data set. The upper scale limit of the ΔL* axis is 43.0, the upper scale limit of the Δa* axis is 4.13, and the upper scale limit of the Δb* axis is –3.67.

Figure 12. The plots of the predicted colorimetric data of the 225 grays in the three-dimensional space. The CIELAB coordinate of the aim gray in the diagram is displayed by □.

gray in colorimetric units.; and (2) the predicted colorimetric data do not have the ideal normal distribution.

In order to determine the three axes of the ellipsoid, an Analysis of Principal Components was performed by using the JMP program. The three components have a value of 1.25, 0.96, and 0.79. These values are variances. In order to obtain numbers that are proportional to the length of the axes, the square root of these variances must be taken. The length of the three principal axes are therefore 1.12, 0.98, and 0.89. If they were identical, the shape would be spherical. Since the ratio between the length of the largest and the shortest axes is close to one (1.26), the ellipsoid is close to a sphere.

Albeit the JMP program itself has no capability to draw the three-dimensional contours around the entire data to underscore its ellipsoidal shape, it can encircle the data located in the two-dimensional space with an ellipse of diverse probability densities. The probability distribution that involves two or more variables is known as joint probability distribution.[1] The joint probability distribution of only two variables is said to be a bivariate distribution.[2] In Figures 13-15, the contours of the ellipses of 95% and 99% probability densities are defined from the means and standard deviations of the L*, a*, and b* data.[3] Of all the 225 CIELAB coordinates, the eight grays, that are located outside the inner ellipse, have the probability density of less than 95% ; nonetheless, the 225 grays, that all are located inside the outer ellipse, have the probability density of greater than 99%. The data points falling out of the inner 95% density ellipse are labeled with their ranks (See Table C1 in Appendix C) and emphasized with a heavy X-mark, while a bold cross signifies the data falling out of the inner 95% density ellipse in the unshown third dimension.

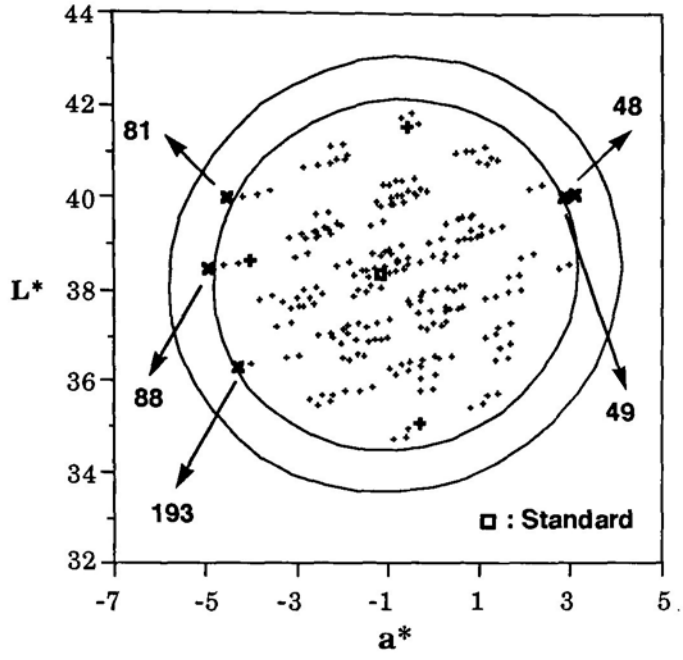

Figure 13. The plots of the a* data against the L* data encompassed with the inner 95% and outer 99% density ellipses.

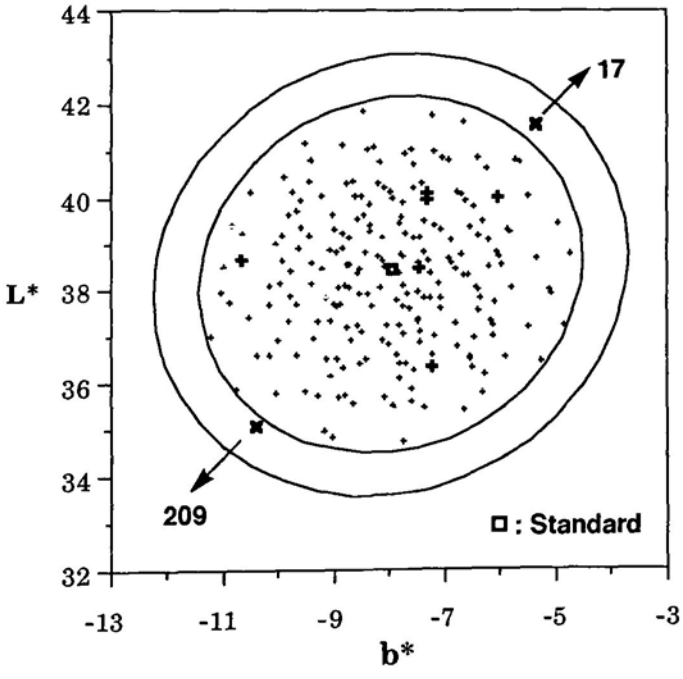

Figure 14. The plots of the b* data against the L* data encompassed with the inner 95% and outer 99% density ellipses.

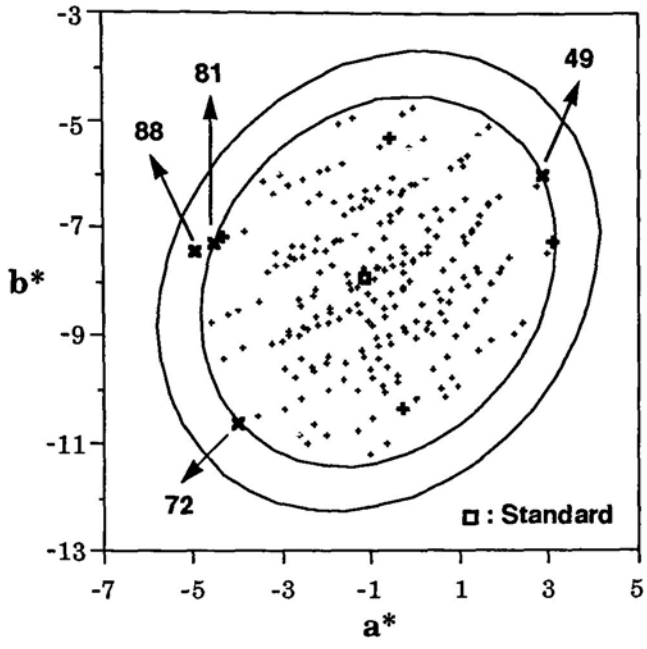

Figure 15. The plots of the a* data against the b* data encompassed with the inner 95% and outer 99% density ellipses.

To find out whether dot gain variations or SID variations contribute more to the total color variation, the ΔE^*_{ab} and ΔC^*_{ab} values in Table 7 are averaged.

From the average ΔE^*_{ab} and ΔC^*_{ab} figures, changing SID levels by ± 0.1 results in a slightly higher degree of color variation of the aim gray than varying dot area by ± 2% . Cyan dot area or SID variation produces the most color variation in the aim gray. Cyan, therefore, requires theoretically a tighter control. However, the differences among the ΔE^*_{ab} and ΔC^*_{ab} figures are very small. Hence, color variations of the aim gray caused by varying dot areas or SIDs are, on average, similar for all three process inks.

Table 7

Comparisons among the ΔE^*_{ab} and ΔC^*_{ab} figures of the colorimetric data due to altering cyan, magenta, and/or yellow dot areas and SIDs

Change in Dot Area	ΔE^*_{ab}	ΔC^*_{ab}	Change in SID	ΔE^*_{ab}	ΔC^*_{ab}
-2% DAs of C, M, & Y	1.55	0.83	**-0.1 SIDs of C, M, & Y**	2.15	0.33
-2% DAs of C & M	2.05	1.46	**-0.1 SIDs of C & M**	2.17	1.30
-2% DAs of C & Y	2.08	1.93	**-0.1 SIDs of C & Y**	2.16	1.81
-2% DA of M & Y	1.82	1.63	**-0.1 SID of M & Y**	2.27	2.06
-2% DAs of C	2.09	1.97	**-0.1 SIDs of C**	2.75	2.58
-2% DA of M	1.83	1.67	**-0.1 SID of M**	1.99	1.80
-2% DA of Y	1.31	1.31	**-0.1 SID of Y**	1.88	1.88
+2% DA of Y	1.31	1.31	**+0.1 SID of Y**	1.61	1.56
+2% DA of M	1.85	1.69	**+0.1 SID of M**	1.39	1.14
+2% DAs of C	2.10	1.98	**+0.1 SIDs of C**	1.73	1.35
+2% DA of M & Y	1.83	1.64	**+0.1 SID of M & Y**	2.37	2.10
+2% DAs of C & Y	2.12	1.97	**+0.1 SIDs of C & Y**	1.79	1.24
+2% DAs of C & M	2.02	1.44	**+0.1 SIDs of C & M**	2.32	1.81
+2% DAs of C, M, & Y	1.54	0.37	**+0.1 SIDs of C, M, & Y**	2.25	0.69
average	1.82	1.51	**average**	2.06	1.55

To test the hypotheses previously formulated in Chapter 5, the statistical technique of TWOWAY ANOVA by the MINITAB program was employed. The outcomes are contained in Appendix D. The calculated F values of each individual collection of the L*, a*, and b* data sets, are greater than the critical F value of a 99% confidence limit. Thus, there are significant differences within each set of the L*, a*, and b* data. The computed F value of the ΔE^*_{ab} data is less than the critical F value of a 99% confidence limit. This statistically declares that there are no significant color differences due to either varying SID or dot gain among the 225 grays within a 99% confidence interval.

Endnotes for Chapter 6

[1]David R. Anderson, Dennis J. Sweeney, and Thomas A. Williams, "Probability Distributions," in *Introduction to Statistics: An Applications Approach* (St. Paul, Minnesota: West Publishing, 1981), 111-13.

[2]Stuart L. Meyer, "Miscellaneous Other Probability Distributions and Some Examples," in *Data Analysis for Scientists and Engineers* (New York: John Wiley & Sons, 1975), 288-90.

[3]Ibid.

Chapter 7

Summary and Conclusions

On the premise that the mathematical models; the GRL Trapping model, the GRL Dot Gain model, and the Yule-Nielsen modified Spectral Neugebauer model, all together can accurately predict the color of the three-color overprint halftone gray from the measured spectral reflectances of the eight Neugebauer Primaries, the FIPP SID and dot gain specifications applied to the Gretag CMS3 gray have been successfully transformed into the colorimetric specification.

When the three-color overprint halftone gray (75% cyan, 62% magenta, and 60% yellow) is printed at 1.46 cyan SID, 1.43 magenta SID, and 1.24 yellow SID with 14% cyan apparent dot gain, 17% magenta apparent dot gain, and 18% yellow apparent dot gain, the correspondent predicted CIELAB coordinate of this aim gray is 38.41 in the L* dimension, -1.08 in the a* dimension, and -7.89 in the b* dimension. By varying the above apparent dot areas of the aim gray within the ± 2% FIPP standardized tolerance window and printing this aim gray to the FIPP standardized SID tolerance window of ± 0.1, a collection of the 225 three-color overprint grays was obtained. The resulting color tolerance ellipsoid has the L* scale ranging from 34.74 to 41.88, the a* scale ranging from -4.88 to 3.17, and the b* scale

ranging from -11.18 to -4.67. The largest deviation of one of these grays from the aim gray is 4.7 ΔE*ab units. The color variations of the aim gray resulting from the changes in SID levels or dot areas are not statistically different at a 99% confidence level. Altering ± 2% dot area of any ink in the aim gray yields the average ΔE^*_{ab} figure of 1.82 and the average ΔC^*_{ab} figure of 1.51. The average ΔE^*_{ab} figure and the average ΔC^*_{ab} figure resulting from a change of ± 0.1 SID of any ink are 2.06 and 1.55, respectively.

Conclusions about the Hypotheses

(1) *Neutrality of Aim Gray*:

The aim gray has the predicted a* value of -1.08 and the predicted b* value of -7.89. The CIE Chroma difference, ΔC^*_{ab}, between this aim gray and the theoretical one is equal to 7.96. Therefore, the hypothesis that " The CIE Chroma of an overprint of 75% cyan dot area, 62% magenta dot area, and 60% yellow dot area, printed to the FIPP specifications for printing at 150 line screen on coated paper and with positive-working plate is less than the just noticeable difference of 2." is rejected.

(2) *Maximum CIELAB Deviation from Aim*:

The maximum ΔE^*_{ab} between one of the 225 grays and the aim gray amounts to 4.74; consequently, the hypothesis that " The largest CIE ΔE^*_{ab} values between the gray produced by printing to the FIPP aim values of solid ink densities and dot gain and all the other near grays produced by the FIPP

tolerances for solid ink densities and dot gain are less than 6 ΔE^*_{ab} units." is accepted.

(3) *Uniformity of Deviations from Aim*:

The computed ΔE^*_{ab} values range from 0.25 to 4.74 with a standard deviation of 0.9. The hypothesis that " All the ΔE^*_{ab} values between the aim gray and the near grays are the same within 2 ΔE^*_{ab} units." is, therefore, rejected.

This hypothesis was formulated to test whether the data points are located more or less the same distance around the aim gray. Instead, it was found that the data points are evenly scattered in a cluster around the aim gray. Therefore, a different question could be asked about the uniformity of deviations from the aim gray: Are the three axes of the cluster of data points the same? As the analysis of Principal Components showed, the ratio of the length of the largest to the shortest axes is close to one (1.26). Thus, the shape of the ellipsoid is almost spherical.

(4) *Equivalence of Traditional and Colorimetric Tolerances*:

The models from multiple regression analyses that describe the relationship between the colorimetric data and the densitometric parameters, dot area and SID, were successfully derived. It proved that it is possible to determine colorimetric specifications that are equivalent to the traditional densitometric specifications. For the conditions chosen for this study (FIPP specifications), one could state that the aim gray should be printed within a tolerance of 5 ΔE^*_{ab} units. Such a colorimetric specification

is essentially identical to the FIPP specifications for the gray of 75% cyan, 62% magenta, and 60% yellow. The hypothesis that "The ellipsoidal CIELAB tolerances can be defined so that they are equivalent (within 2 units of the CIE ΔE^*_{ab}) to tolerances based on specifications of solid ink density tolerances and dot gain tolerances." is then accepted.

Recommendations for Further Investigation

(1) The colorimetric specification in this study is based on (a) using the Gretag CMS3 three-color overprint gray for a press control and (b) printing with the European CEI 30–89 process inks at 150 line screen on coated paper with positive-working plate. This research work could be extended to other printing conditions and materials of interest.

(2) This study did not take account of a black ink. However, adding black to the specifications does not change anything that has been done so far. This is even true when GCR (Gray Component Replacement) is used because in this case, saturated colors still need to be controlled. All that would have to be done is to add a black tint patch that has the same density as the three-color overprint gray patch and put specification of L* on it.

(3) It might be interesting to study what happen to other colors when the color variation of 75%C-62%M-60%Y gray remains within 5 ΔE^*_{ab} units.

List of References

American National Standards Institute. *American National Standard for Photography (Sensitometry)–Density Measurements–Spectral Conditions*. ANSI/ASC PH2.18. New York: American National Standards Institute, 1984.

American Society for Testing and Materials. "Standard Method for Computing the Colors of Objects by Using the CIE System." in *ASTM Standards on Color and Appearance Measurement*. ASTM Designation: E308–85. 2d ed. Philadelphia, PA: American Society for Testing and Materials, 1987.

Anderson, David R., Dennis J. Sweeney, and Thomas A. Williams. "Probability Distributions." in *Introduction to Statistics: An Applications Approach*. St. Paul, MN: West Publishing, 1981.

Ba'adarani, Amal A. "A Study on Doubling in the Offset Printing Process." M.S. thesis, Rochester Institute of Technology, 1989.

Billmeyer, Fred W. , Jr., and Max Saltzman. "Describing Color?." in *Principles of Color Technology*. 2d ed. New York: John Wiley & Sons, 1981.

Bulger, Mary Louise. " A Colorimetric Analysis of Color Variation Due to Changes in Simulated Ink Trapping." M.S. thesis, Rochester Institute of Technology, 1988.

Chen, Jang-fun. "An Investigation of Color Variation As a Function of Register in Dot-on-Dot Multicolor Halftone Printing." in *TAGA Proceedings*. Rochester, NY: Technical Association of the Graphic Arts, 1984, 315-33.

Chung, Robert, and John Compton. "A Colorimetric Method for Visualizing and Determining Color Tolerances of Printed Colors." in *TAGA Proceedings*. Rochester, NY: Technical Association of the Graphic Arts, 1991, 119-129.

Commission Internationale de l' Éclairage (CIE). *Colorimetry*. Pub. No. 15.2, 2d. ed. Vienna, Austria: Central Bureau of the CIE, 1986.

Deutsche Forschungsgesellschaft für Druck- und Reproduktionstechnik E.V. (FOGRA. *BVD/FOGRA Standardisation of Offset Printing*. FOGRA Praxis Report Nr. 30, rev. 2d ed. Munich, West Germany: Deutsche Forschungsgesellschaft für Druck- und Reproduktionstechnik E.V, 1984.

Dowdy, Shirley, and Stanley Wearden. *Statistics for Research*. 2d. ed. New York:John Wiley & Sons, 1991.

EMPA/UGRA. *The Spectral Reflectance Values for Ink Colors and Paper for Multi-Color Printing*. CEI 30–89. St.Gallen, Switzerland: EMPA/UGRA, Dec 1992. Fax Transmission.

Field, Gary G. *Color and Its Reproduction*. Pittsburgh, PA: Graphic Arts Technical Foundation, 1988.

Gretag Company. *Gretag Sticker with Recommended Solid and Dot Gain Aim Values and Tolerances*. Gretag Product No. 98.16.75 KL8511. Switzerland: Gretag Company, n.d.

Harrington, Steven J. "An Analytical Solution to the Neugebauer Equations." in *TAGA Proceedings*. Rochester, NY: Technical Association of the Graphic Arts, 1991, 144-53.

Hunt, R. W. G. "Colour Vision." in *Measuring Colour*. Ellis Horwood Series in Applied Science and Industrial Technology. 2d ed. New York: John Wiley & Sons, 1987.

Hunter, Richard S., and Richard W. Harold, eds. *The Measurement of Appearance*. 2d ed. New York: John Wiley & Sons, 1987.

International Federation of the Periodical Press (FIPP). *Specifications for European Offset Printing of Periodicals*. rev. 2d ed. United Kingdom: International Federation of the Periodical Press, 1988.

JMP Ver. 2. SAS Institute, Cary, NC.

Link, Dawn Leslie. "An Investigation of the Effects of Screen Ruling and Dot Structure Have on Dot Gain on Offset Newsprint." M.S. thesis, Rochester Institute of Technology, 1986.

Malikhao, Patchanee. " The Application of CIELAB to Study Trapping Efficiency." M.S. thesis, Rochester Institute of Technology, 1988.

Meyer, Stuart L. "Miscellaneous Other Probability Distributions and Some Examples." in *Data Analysis for Scientists and Engineers.* New York: John Wiley & Sons, 1975.

Mudge, James B. "A Study of the Effect of Lithographic Press Speed on Dot Gain." M.S. thesis, Rochester Institute of Technology, 1991.

Pearson, Milton. "n Value for General Conditions." in *TAGA Proceedings* Rochester, NY: Technical Association of the Graphic Arts, 1980, 415–25.

Southworth, Miles and Donna Southworth, eds. "Densitometry." in *Quality and Productivity in the Graphic Arts.* New York: Graphic Arts Publishing, 1989.

Stamm, Scott. "A Colorimetric Investigation of Color Tolerances." M.S. thesis, Rochester Institute of Technology, 1980).

Sun, Kuang-Hua. "A Study of Mechanical Dot Gain for Different Dot Shapes Based on the Border Zone Theory." M.S. thesis, Rochester Institute of Technology, 1991.

Viggiano, J. A. Stephen. "Modeling the Color of Multi-Colored Halftones." in *TAGA Proceedings.* Rochester, NY: Technical Association of the Graphic Arts, 1990, 44-62.

_____. "The GRL Dot Gain Model." in *TAGA Proceedings.* Rochester, NY: Technical Association of the Graphic Arts, 1983, 423-39.

Appendices

Appendix A

(1) Color Matching Functions of the CIE 2° and 10° Standard Observers

(2) Spectral Products – Status T Densities

(3) Spectral Reflectances Values of the Eight Neugebauer Primaries

Table A1

Color Matching Functions (CMFs) of the 2°, 1931 and 10°, 1964 Standard Observers for wavelengths (λ) of 380 nm to 760 nm at 10 nm intervals

λ	2°, 1931 CMF			10°, 1964 CMF		
(nm)	$\bar{x}$	$\bar{y}$	$\bar{z}$	$\bar{x}_{10}$	$\bar{y}_{10}$	$\bar{z}_{10}$
380	0.0014	0.0000	0.0065	0.0002	0.0000	0.0007
390	0.0042	0.0001	0.0201	0.0024	0.0003	0.0105
400	0.0143	0.0004	0.0679	0.0191	0.0020	0.0860
410	0.0435	0.0012	0.2074	0.0847	0.0088	0.3894
420	0.1344	0.0040	0.6456	0.2045	0.0214	0.9725
430	0.2839	0.0116	1.3856	0.3147	0.0387	1.5535
440	0.3483	0.0230	1.7471	0.3837	0.0621	1.9673
450	0.3362	0.0380	1.7721	0.3707	0.0895	1.9948
460	0.2908	0.6000	1.6692	0.3023	0.1282	1.7454
470	0.1954	0.0910	1.2876	0.1956	0.1852	1.3176
480	0.0956	0.1390	0.8130	0.0805	0.2536	0.7721
490	0.0320	0.2080	0.4652	0.0162	0.3391	0.4153
500	0.0049	0.3230	0.2720	0.0038	0.4608	0.2185
510	0.0093	0.5030	0.1582	0.0375	0.6067	0.1120
520	0.0633	0.7100	0.0782	0.1177	0.7618	0.0607
530	0.1655	0.8620	0.0422	0.2365	0.8752	0.0305
540	0.2904	0.9540	0.0203	0.3768	0.9620	0.0137
550	0.4334	0.9950	0.0087	0.5298	0.9918	0.0040
560	0.5945	0.9950	0.0039	0.7052	0.9973	0.0000
570	0.7621	0.9520	0.0021	0.8787	0.9556	0.0000
580	0.9163	0.8700	0.0017	1.0142	0.8689	0.0000
590	1.0263	0.7570	0.0011	1.1185	0.7774	0.0000
600	1.0622	0.6310	0.0008	1.1240	0.6583	0.0000
610	1.0026	0.5030	0.0003	1.0305	0.5280	0.0000
620	0.8544	0.3810	0.0002	0.8563	0.3981	0.0000
630	0.6424	0.2650	0.0000	0.6475	0.2835	0.0000
640	0.4479	0.1750	0.0000	0.4316	0.1798	0.0000
650	0.2835	0.1070	0.0000	0.2683	0.1076	0.0000
660	0.1649	0.0610	0.0000	0.1526	0.0603	0.0000
670	0.0874	0.0320	0.0000	0.0813	0.0318	0.0000
680	0.0468	0.0170	0.0000	0.0409	0.0159	0.0000
690	0.0227	0.0082	0.0000	0.0199	0.0077	0.0000

Table A1 (continued).

λ	2°, 1931 CMF			10°, 1964 CMF		
(nm)	$\bar{x}$	$\bar{y}$	$\bar{z}$	$\bar{x}_{10}$	$\bar{y}_{10}$	$\bar{z}_{10}$
700	0.0114	0.0041	0.0000	0.0096	0.0037	0.0000
710	0.0058	0.0021	0.0000	0.0046	0.0018	0.0000
720	0.0029	0.0010	0.0000	0.0022	0.0008	0.0000
730	0.0014	0.0005	0.0000	0.0010	0.0004	0.0000
740	0.0007	0.0002	0.0000	0.0005	0.0002	0.0000
750	0.0003	0.0001	0.0000	0.0003	0.0001	0.0000
760	0.0002	0.0001	0.0000	0.0001	0.0000	0.0000

Table A2

Spectral Products – Status T Densities

λ (nm)	Blue		Green		Red	
	Relative Power x 10^{-3}	Relative Log Power	Relative Power x 10^{-3}	Relative Log Power	Relative Power x 10^{-3}	Relative Log Power
340	< 0.010	< 1.000	–	–	–	–
350	0.010	1.000	–	–	–	–
360	0.020	1.301	–	–	–	–
370	0.100	2.000	–	–	–	–
380	0.300	2.477	–	–	–	–
390	1.500	3.176	–	–	–	–
400	6.000	3.778	–	–	–	–
410	17.000	4.230	–	–	–	–
420	40.000	4.602	–	–	–	–
430	60.000	4.778	–	–	–	–
440	82.000	4.914	–	–	–	–
450	94.000	4.973	–	–	–	–
460	100.000	5.000	–	–	–	–
470	97.000	4.987	< 0.010	< 1.000	–	–
480	85.000	4.929	1.000	3.000	–	–
490	65.000	4.813	5.000	3.699	–	–
500	40.000	4.602	30.000	4.477	–	–
510	18.000	4.255	68.000	4.833	–	–
520	5.000	3.699	92.000	4.694	–	–
530	0.200	2.301	100.000	5.000	–	–
540	0.040	1.602	88.000	4.944	–	–
550	< 0.010	< 1.000	66.000	4.820	–	–
560	–	–	42.000	4.623	< 0.010	< 1.000
570	–	–	22.000	4.342	0.060	1.778
580	–	–	9.000	3.954	0.450	2.653
590	–	–	2.500	3.398	30.000	4.477
600	–	–	0.700	2.845	100.000	5.000
610	–	–	0.090	1.954	85.000	4.929
620	–	–	0.010	1.000	55.000	4.740
630	–	–	< 0.010	< 1.000	25.000	4.398
640	–	–	–	–	10.000	4.000
650	–	–	–	–	5.000	3.699

Table A2 (continued).

λ (nm)	Blue		Green		Red	
	Relative Power x 10^{-3}	Relative Log Power	Relative Power x 10^{-3}	Relative Log Power	Relative Power x 10^{-3}	Relative Log Power
660	–	–	–	–	1.500	3.176
670	–	–	–	–	0.500	2.699
680	–	–	–	–	0.300	2.477
690	–	–	–	–	0.150	2.176
700	–	–	–	–	0.050	1.699
710	–	–	–	–	0.010	1.000
720	–	–	–	–	< 0.010	< 1.000
730	–	–	–	–	–	–
740	–	–	–	–	–	–
750	–	–	–	–	–	–
760	–	–	–	–	–	–
770	–	–	–	–	–	–

Table A3. Spectral reflectance values for colors of the CEI 30-89 process inks and paper for multi-color printing

λ (nm)	C	M	Y	C/M (Blue)	C/Y (Green)	M/Y (Red)	C/M/Y (3-Color)	Paper (White)
380	0.080	0.258	0.053	0.044	0.017	0.024	0.011	0.720
390	0.172	0.225	0.040	0.084	0.022	0.017	0.013	0.741
400	0.293	0.201	0.034	0.118	0.024	0.015	0.014	0.759
410	0.397	0.196	0.031	0.142	0.025	0.014	0.014	0.773
420	0.420	0.199	0.031	0.150	0.024	0.015	0.014	0.787
430	0.482	0.210	0.035	0.170	0.027	0.017	0.016	0.799
440	0.586	0.224	0.039	0.201	0.033	0.020	0.020	0.808
450	0.644	0.220	0.049	0.201	0.043	0.025	0.024	0.819
460	0.661	0.193	0.064	0.178	0.057	0.031	0.028	0.828
470	0.666	0.159	0.083	0.148	0.074	0.034	0.030	0.834
480	0.657	0.125	0.118	0.117	0.109	0.040	0.034	0.840
490	0.634	0.097	0.216	0.092	0.197	0.049	0.042	0.847
500	0.597	0.072	0.394	0.070	0.339	0.051	0.044	0.868
510	0.539	0.048	0.597	0.046	0.439	0.040	0.036	0.870
520	0.456	0.032	0.737	0.029	0.427	0.026	0.024	0.879
530	0.361	0.025	0.799	0.022	0.352	0.022	0.019	0.882
540	0.262	0.024	0.820	0.017	0.259	0.021	0.016	0.885
550	0.172	0.020	0.829	0.012	0.168	0.016	0.011	0.887
560	0.099	0.015	0.833	0.009	0.098	0.012	0.008	0.891
570	0.059	0.016	0.837	0.008	0.058	0.012	0.007	0.893
580	0.042	0.034	0.846	0.009	0.041	0.031	0.009	0.893
590	0.036	0.194	0.865	0.017	0.034	0.198	0.018	0.895
600	0.032	0.478	0.877	0.021	0.028	0.488	0.023	0.898
610	0.029	0.691	0.882	0.021	0.026	0.704	0.025	0.899
620	0.030	0.801	0.886	0.022	0.026	0.811	0.026	0.900
630	0.031	0.845	0.892	0.025	0.030	0.857	0.029	0.901
640	0.032	0.862	0.895	0.026	0.033	0.874	0.031	0.901

Table A3 (continued).

λ (nm)	C	M	Y	C/M (Blue)	C/Y (Green)	M/Y (Red)	C/M/Y (3-color)	Paper (White)
650	0.037	0.871	0.898	0.033	0.038	0.881	0.037	0.902
660	0.044	0.873	0.895	0.042	0.048	0.884	0.046	0.902
670	0.047	0.876	0.896	0.044	0.050	0.886	0.048	0.903
680	0.045	0.876	0.894	0.041	0.046	0.883	0.045	0.904
690	0.042	0.878	0.893	0.038	0.040	0.882	0.041	0.904
700	0.036	0.879	0.894	0.036	0.032	0.888	0.036	0.904
710	0.032	0.881	0.893	0.033	0.030	0.892	0.033	0.902
720	0.034	0.883	0.895	0.029	0.035	0.895	0.034	0.900

Note: Because the spectral reflcetance values of the three-color overprint C/M/Y were not provided by EMPA/UGRA, the values listed in this table were computed by Mr. J.A. Stephen Viggiano from the available data in this table.

Appendix B

Calculations of Tint Density with the Murray-Davies Equation and Dot Gain Figure at 50% Dot Area with the GRL Dot Gain Model

(1) Calculations of tint densities from FIPP standardized SID and apparent dot areas (ADA) by employing the Murray-Davies formula:

(B1)
$$ADA = \frac{1-10^{-Dt}}{1-10^{-Ds}} \quad \text{or}$$

$$Dt = -\log [\, 1-ADA(1-10^{-Ds}) \,]$$

where ADA = Apparent dot area
Dt = Density of the tint area
Ds = Density of the solid area

(ADA of printed Cyan = 89% (75%+14%) and Cyan SID = 1.4576)

$$\begin{aligned} Dt \text{ of Cyan} &= -\log [\, 1- 0.89 (1-10^{-1.4576}) \,] \\ &= -\log 1.410 \\ &= 0.8507 \end{aligned}$$

With the same computational means applied to Magenta having ADA of 79% (62%+17%) and SID of 1.4335 and Yellow having ADA of 78% (60%+18%) and SID of 1.240, Dt of Magenta and Dt of Yellow are 0.6214 and 0.5771, respectively.

To obtain mechanical dot area on paper (DA_p) corresponding to ADA, the VMODEL.EXE was operated. The 75% cyan dot area on film was kept changing until Dt of 0.8507 was the consequence. The predicted cyan DA_p of 0.7678 was recorded for the dot gain calculations. The identical performance was conducted on the 62% magenta dot area on film and the 60% yellow dot area on film. The results were the magenta DA_p of 0.6282 and the yellow DA_p of 0.6199.

(2) Calculations of the amount of dot gain at 50% dot area ($DG_{50\%}$) by utilizing the GRL dot gain model:

(B2)
$$DA_p = DA_f + 2\, DG_{50\%} [DA_f (1-DA_f)]^{1/2} \quad \text{or}$$

$$DG_{50\%} = \frac{DA_p - DA_f}{2\,[\,DA_f(1-DA_f)\,]^{1/2}}$$

(DA_p of Cyan = 76.78% and DA_f of Cyan =75%)

$$DG_{50\%} = \frac{0.7678 - 0.75}{2\,[\,0.75\,(1-0.75)\,]^{1/2}}$$

$$= 0.0206$$

With the same computational means applied to Magenta having DA_p of 0.6282 and 62% DA_f and Yellow having DA_p of 0.6199 and 60% DA_f of, $DG_{50\%}$ figures of Magenta and of Yellow are 0.0084 and 0.0364, respectively. These dot gain figures were then edited into the VMODEL.DEF file.

Appendix C

(1) Predicted CIELAB Coordinates of the 225 Three-Color Halftone Grays and Their Color Differences

(2) Predicted Status E Densities of the 225 Three-Color Halftone Grays

(3) Predicted CIELAB Coordinates of the Status E Solid Ink Densities of Cyan, Magenta, and Yellow Inks

Table C1. Colorimetric data of 15 C-M-Y dot area combinations printed at 15 combinations of C-M-Y solid ink densities according to FIPP SID and dot gain specifications

SID Combination		C/M/Y (%)	L*	a*	b*	ΔL*	Δa*	Δb*	ΔE^*_{ab}
01(LLL)	1	73 / 60 / 58	41.88	-0.39	-8.41	3.47	0.69	-0.52	3.58
	2	73 / 60 / 60	41.51	-0.66	-7.15	3.40	0.42	0.74	3.50
SID:	3	73 / 62 / 58	41.15	1.20	-8.78	2.74	2.28	-0.89	3.67
Dr of C = 1.3578	4	73 / 62 / 60	41.08	0.93	-7.53	2.67	2.01	0.36	3.36
Dg of M= 1.3335	5	75 / 60 / 58	41.20	-1.95	-9.47	2.79	-0.87	-1.58	3.32
Db of Y = 1.1409	6	75 / 60 / 60	41.13	-2.22	-8.22	2.72	-1.14	-0.33	2.97
	7	75 / 62 / 58	40.48	-0.37	-9.84	2.07	0.71	-1.95	2.93
C^*_{ab}:	8	**75 / 62 / 60**	**40.40**	**-0.64**	**-8.59**	**1.99**	**0.44**	**-0.70**	**2.16**
	9	75 / 62 / 62	40.33	-0.91	-7.34	1.92	0.17	0.55	2.01
min.: 7.18 **(2)**	10	75 / 64 / 60	39.68	0.95	-8.97	1.27	2.03	-1.08	2.63
max.: 10.03 **(14)**	11	75 / 64 / 62	39.61	0.69	-7.73	1.20	1.77	0.16	2.14
	12	77 / 62 / 60	39.74	-2.24	-9.64	1.33	-1.16	-1.75	2.49
Illuminant: D_{50}	13	77 / 62 / 62	39.66	-2.52	-8.40	1.25	-1.44	-0.51	1.97
CIE Observer: 10°	14	77 / 64 / 60	39.02	-0.65	-10.01	0.61	0.43	-2.12	2.25
	15	77 / 64 / 62	38.95	-0.93	-8.78	0.54	0.15	-0.89	1.05
		min.	38.95	-2.52	-10.01	0.54	-1.44	-2.12	1.05
		max.	41.88	1.20	-7.15	3.47	2.28	0.74	3.67
		avg.	40.41	-0.65	-8.59	2.00	0.43	-0.70	2.67
		stdev	0.95	1.22	0.90	0.95	1.22	0.90	0.75

Note : The L*, a*, and b* values of the (aim) standard are 38.41, -1.08, and -7.89, respectively.

Table C1 (continued).

SID Combination		C/M/Y (%)	L*	a*	b*	ΔL*	Δa*	Δb*	ΔE^*_{ab}
02(LLA)	**16**	73 / 60 / 58	41.64	-0.26	-6.61	3.23	0.82	1.28	3.57
	17	73 / 60 / 60	41.56	-0.51	-5.27	3.15	0.57	2.62	4.14
SID:	**18**	73 / 62 / 58	40.91	1.34	-6.99	2.50	2.42	0.90	3.59
Dr of C = 1.3577	**19**	73 / 62 / 60	40.83	1.09	-5.67	2.42	2.17	2.22	3.94
Dg of M= 1.3335	**20**	75 / 60 / 58	40.96	-1.82	-7.67	2.55	-0.74	0.22	2.66
Db of Y = 1.2408	**21**	75 / 60 / 60	40.88	-2.09	-6.34	2.47	-1.01	1.55	3.09
	22	75 / 62 / 58	40.24	-0.23	-8.05	1.83	0.85	-0.16	2.02
C^*_{ab}:	**23**	**75 / 62 / 60**	**40.16**	**-0.49**	**-6.73**	**1.75**	**0.59**	**1.16**	**2.18**
	24	75 / 62 / 62	40.08	-0.74	-5.41	1.67	0.34	2.48	3.01
min.: 5.29 **(17)**	**25**	75 / 64 / 60	39.44	1.13	-7.11	1.03	2.21	0.78	2.56
max.: 8.17 **(29)**	**26**	75 / 64 / 62	39.36	0.88	-5.81	0.95	1.96	2.08	3.01
	27	77 / 62 / 60	39.48	-2.09	-7.78	1.07	-1.01	0.11	1.48
Illuminant: D_{50}	**28**	77 / 62 / 62	39.40	-2.35	-6.47	0.99	-1.27	1.42	2.15
CIE Observer: 10°	**29**	77 / 64 / 60	38.77	-0.48	-8.16	0.36	0.60	-0.27	0.75
	30	77 / 64 / 62	38.69	-0.74	-6.86	0.28	0.34	1.03	1.12
		min	38.69	-2.35	-8.16	0.28	-1.27	-0.27	0.75
		max.	41.64	1.34	-5.27	3.23	2.42	2.62	4.14
		avg.	40.16	-0.49	-6.73	1.75	0.59	1.16	2.62
		stdev.	0.95	1.22	0.93	0.95	1.22	0.93	1.01

Note : The L*, a*, and b* values of the (aim) standard are 38.41, -1.08, and -7.89, respectively.

Table C1 (continued).

SID Combination		C/M/Y (%)	L*	a*	b*	ΔL*	Δa*	Δb*	ΔE^*_{ab}
03(LAL)	**31**	73 / 60 / 58	41.08	0.80	-8.35	2.67	1.88	-0.46	3.30
	32	73 / 60 / 60	41.01	0.54	-7.11	2.60	1.62	0.78	3.16
SID:	**33**	73 / 62 / 58	40.32	2.45	-8.71	1.91	3.53	-0.82	4.10
Dr of C = 1.3577	**34**	73 / 62 / 60	40.25	2.19	-7.49	1.84	3.27	0.40	3.77
Dg of M= 1.4335	**35**	75 / 60 / 58	40.40	-0.76	-9.39	1.99	0.32	-1.50	2.51
Db of Y = 1.1409	**36**	75 / 60 / 60	40.33	-1.03	-8.16	1.92	0.05	-0.27	1.94
	37	75 / 62 / 58	39.65	0.88	-9.76	1.24	1.96	-1.87	2.98
C^*_{ab}:	**38**	**75 / 62 / 60**	**39.58**	**0.61**	**-8.54**	**1.17**	**1.69**	**-0.65**	**2.16**
	39	75 / 62 / 62	39.51	0.34	-7.31	1.10	1.42	0.58	1.89
min.: 7.13 **(32)**	**40**	75 / 64 / 60	38.83	2.26	-8.91	0.42	3.34	-1.02	3.52
max.: 9.96 **(44)**	**41**	75 / 64 / 62	38.76	1.99	-7.70	0.35	3.07	0.19	3.10
	42	77 / 62 / 60	38.91	-0.99	-9.58	0.50	0.09	-1.69	1.77
Illuminant: D_{50}	**43**	77 / 62 / 62	38.85	-1.27	-8.36	0.44	-0.19	-0.47	0.67
CIE Observer: 10°	**44**	77 / 64 / 60	38.17	0.65	-9.94	-0.24	1.73	-2.05	2.69
	45	77 / 64 / 62	38.10	0.37	-8.74	-0.31	1.45	-0.85	1.71
		min.	38.10	-1.27	-9.94	-0.31	-0.19	-2.05	0.67
		max.	41.08	2.45	-7.11	2.67	3.53	0.78	4.10
		avg.	39.58	0.60	-8.54	1.17	1.68	-0.65	2.62
		stdev.	0.96	1.24	0.89	0.96	1.24	0.89	0.93

Note : The L*, a*, and b* values of the (aim) standard are 38.41, -1.08, and -7.89, respectively.

Table C1 (continued).

SID Combination		C/M/Y (%)	L*	a*	b*	ΔL*	Δa*	Δb*	ΔE^*_{ab}
04(LAA)	**46**	73 / 60 / 58	40.86	1.49	-6.86	2.45	2.57	1.03	3.70
	47	73 / 60 / 60	40.78	1.26	-5.57	2.37	2.34	2.32	4.06
SID:	**48**	73 / 62 / 58	40.11	3.17	-7.25	1.70	4.25	0.64	4.62
Dr of C = 1.3577	**49**	73 / 62 / 60	40.04	2.94	-5.97	1.63	4.02	1.92	4.74
Dg of M= 1.4335	**50**	75 / 60 / 58	40.18	-0.07	-7.93	1.77	1.01	-0.04	2.04
Db of Y = 1.2408	**51**	75 / 60 / 60	40.10	-0.31	-6.64	1.69	0.77	1.25	2.24
	52	75 / 62 / 58	39.43	1.60	-8.31	1.02	2.68	-0.42	2.90
C^*_{ab}:	**53**	**75 / 62/ 60**	**39.35**	**1.36**	**-7.03**	**0.94**	**2.44**	**0.86**	**2.75**
	54	75 / 62 / 62	39.28	1.13	-5.76	0.87	2.21	2.13	3.19
min.: 5.71 **(47)**	**55**	75 / 64 / 60	38.61	3.05	-7.42	0.20	4.13	0.47	4.16
max.: 8.60 **(59)**	**56**	75 / 64 / 62	38.54	2.82	-6.16	0.13	3.90	1.73	4.27
	57	77 / 62 / 60	38.68	-0.24	-8.09	0.27	0.84	-0.20	0.91
Illuminant: D_{50}	**58**	77 / 62 / 62	38.60	-0.48	-6.82	0.19	0.60	1.07	1.24
CIE Observer: 10°	**59**	77 / 64 / 60	37.94	1.44	-8.48	-0.47	2.52	-0.59	2.63
	60	77 / 64 / 62	37.86	1.20	-7.22	-0.55	2.28	0.67	2.44
		min.	37.86	-0.48	-8.48	-0.55	0.60	-0.59	0.91
		max.	40.86	3.17	-5.57	2.45	4.25	2.32	4.74
		avg.	39.36	1.36	-7.03	0.95	2.44	0.86	3.06
		stdev.	0.97	1.25	0.92	0.97	1.25	0.92	1.19

Note : The L*, a*, and b* values of the (aim) standard are 38.41, -1.08, and -7.89, respectively.

Table C1 (continued).

SID Combination		C/M/Y (%)	L*	a*	b*	ΔL*	Δa*	Δb*	ΔE^*_{ab}
05(ALL)	**61**	73 / 60 / 58	40.86	-1.90	-9.37	2.45	-0.82	-1.48	2.98
	62	73 / 60 / 60	40.79	-2.19	-8.11	2.38	-1.11	-0.22	2.64
SID:	**63**	73 / 62 / 58	40.14	-0.34	-9.72	1.73	0.74	-1.83	2.62
Dr of C = 1.4576	**64**	73 / 62 / 60	40.07	-0.63	-8.47	1.66	0.45	-0.58	1.82
Dg of M= 1.3335	**65**	75 / 60 / 58	40.16	-3.53	-10.45	1.75	-2.45	-2.56	3.95
Db of Y = 1.1409	**66**	75 / 60 / 60	40.08	-3.83	-9.19	1.67	-2.75	-1.30	3.47
	67	75 / 62 / 58	39.44	-1.97	-10.80	1.03	-0.89	-2.91	3.21
C^*_{ab}:	**68**	**75 / 62 / 60**	**39.37**	**-2.27**	**-9.55**	**0.96**	**-1.19**	**-1.66**	**2.26**
	69	75 / 62 / 62	39.30	-2.57	-8.31	0.89	-1.49	-0.42	1.79
min.: 8.40 **(62)**	**70**	75 / 64 / 60	38.66	-0.71	-9.91	0.25	0.37	-2.02	2.07
max.: 11.33 **(72)**	**71**	75 / 64 / 62	38.59	-1.00	-8.68	0.18	0.08	-0.79	0.81
	72	77 / 62 / 60	38.68	-3.94	-10.62	0.27	-2.86	-2.73	3.96
Illuminant: D_{50}	**73**	77 / 62 / 62	38.61	-4.25	-9.38	0.20	-3.17	-1.49	3.51
CIE Observer: 10°	**74**	77 / 64 / 60	37.97	-2.39	-10.98	-0.44	-1.31	-3.09	3.39
	75	77 / 64 / 62	37.90	-2.69	-9.75	-0.51	-1.61	-1.86	2.51
		min.	37.90	-4.25	-10.98	-0.51	-3.17	-3.09	0.81
		max.	40.86	-0.34	-8.11	2.45	0.74	-0.22	3.96
		avg.	39.37	-2.28	-9.55	0.96	-1.20	-1.66	2.73
		stdev.	0.95	1.25	0.91	0.95	1.25	0.91	0.89

Note : The L*, a*, and b* values of the (aim) standard are 38.41, -1.08, and -7.89, respectively.

Table C1 (continued).

SID Combination		C/M/Y (%)	L*	a*	b*	ΔL*	Δa*	Δb*	ΔE^*_{ab}
06(ALA)	**76**	73 / 60 / 58	40.75	-2.49	-7.51	2.34	-1.41	0.38	2.76
	77	73 / 60 / 60	40.68	-2.79	-6.18	2.27	-1.71	1.71	3.32
SID:	**78**	73 / 62 / 58	40.03	-0.88	-7.89	1.62	0.20	0.00	1.63
Dr of C = 1.4576	**79**	73 / 62 / 60	39.96	-1.17	-6.57	1.55	-0.09	1.32	2.04
Dg of M= 1.3335	**80**	75 / 60 / 58	40.06	-4.16	-8.58	1.65	-3.08	-0.69	3.56
Db of Y = 1.2408	**81**	75 / 60 / 60	39.98	-4.47	-7.26	1.57	-3.39	0.63	3.79
	82	75 / 62 / 58	39.33	-2.55	-8.96	0.92	-1.47	-1.07	2.04
C^*_{ab}:	**83**	**75 / 62 / 60**	**39.26**	**-2.86**	**-7.65**	**0.85**	**-1.78**	**0.24**	**1.99**
	84	75 / 62 / 62	39.19	-3.15	-6.34	0.78	-2.07	1.55	2.70
min.: 6.67 **(79)**	**85**	75 / 64 / 60	38.54	-1.23	-8.04	0.13	-0.15	-0.15	0.25
max.: 9.84 **(87)**	**86**	75 / 64 / 62	38.47	-1.52	-6.74	0.06	-0.44	1.15	1.23
	87	77 / 62 / 60	38.57	-4.57	-8.72	0.16	-3.49	-0.83	3.59
Illuminant: D_{50}	**88**	77 / 62 / 62	38.50	-4.88	-7.41	0.09	-3.80	0.48	3.83
CIE Observer: 10°	**89**	77 / 64 / 60	37.86	-2.95	-9.10	-0.55	-1.87	-1.21	2.29
	90	77 / 64 / 62	37.78	-3.26	-7.80	-0.63	-2.18	0.09	2.27
		min.	37.78	-4.88	-9.10	-0.63	-3.80	-1.21	0.25
		max.	40.75	-0.88	-6.18	2.34	0.20	1.71	3.83
		avg.	39.26	-2.86	-7.65	0.85	-1.78	0.24	2.49
		stdev.	0.96	1.28	0.93	0.96	1.28	0.93	1.03

Note : The L*, a*, and b* values of the (aim) standard are 38.41, -1.08, and -7.89, respectively.

Table C1 (continued).

SID Combination		C/M/Y (%)	L*	a*	b*	ΔL*	Δa*	Δb*	ΔE^*_{ab}
07(AAL)	**91**	73 / 60 / 58	39.96	-0.60	-9.54	1.55	0.48	-1.65	2.31
	92	73 / 60 / 60	39.89	-0.88	-8.30	1.48	0.20	-0.41	1.55
SID:	**93**	73 / 62 / 58	39.21	1.02	-9.90	0.80	2.10	-2.01	3.01
Dr of C = 1.4576	**94**	73 / 62 / 60	39.15	0.74	-8.68	0.74	1.82	-0.79	2.12
Dg of M= 1.4335	**95**	75 / 60 / 58	39.26	-2.22	-10.61	0.85	-1.14	-2.72	3.07
Db of Y = 1.1409	**96**	75 / 60 / 60	39.19	-2.52	-9.39	0.78	-1.44	-1.50	2.22
	97	75 / 62 / 58	38.51	-0.61	-10.97	0.10	0.47	-3.08	3.12
C^*_{ab}:	**98**	**75 / 62 / 60**	**38.45**	**-0.91**	**-9.75**	**0.04**	**0.17**	**-1.86**	**1.87**
	99	75 / 62 / 62	38.38	-1.20	-8.53	-0.03	-0.12	-0.64	0.65
min.: 8.35 **(92)**	**100**	75 / 64 / 60	37.70	0.72	-10.12	-0.71	1.80	-2.23	2.95
max.: 11.22 **(104)**	**101**	75 / 64 / 62	37.64	0.43	-8.91	-0.77	1.51	-1.02	1.98
	102	77 / 62 / 60	37.76	-2.58	-10.82	-0.65	-1.50	-2.93	3.36
Illuminant: D_{50}	**103**	77 / 62 / 62	37.69	-2.88	-9.61	-0.72	-1.80	-1.72	2.59
CIE Observer: 10°	**104**	77 / 64 / 60	37.02	-0.96	-11.18	-1.39	0.12	-3.29	3.57
	105	77 / 64 / 62	36.95	-1.26	-9.98	-1.46	-0.18	-2.09	2.56
		min	36.95	-2.88	-11.18	-1.46	-1.80	-3.29	0.65
		max.	39.96	1.02	-8.30	1.55	2.10	-0.41	3.57
		avg.	38.45	-0.91	-9.75	0.04	0.17	-1.86	2.46
		stdev.	0.97	1.26	0.90	0.97	1.26	0.90	0.77

Note : The L", a*, and b* values of the (aim) standard are 38.41, -1.08, and -7.89, respectively.

Table C1 (continued).

SID Combination		C/M/Y (%)	L*	a*	b*	ΔL*	Δa*	Δb*	ΔE^*_{ab}
08(AAA)	**106**	73 / 60 / 58	39.93	-0.80	-7.71	1.52	0.28	0.18	1.56
	107	73 / 60 / 60	39.86	-1.08	-6.41	1.45	0.00	1.48	2.07
SID (AIM):	**108**	73 / 62 / 58	39.18	0.88	-8.09	0.77	1.96	-0.20	2.12
Dr of C = 1.4576	**109**	73 / 62 / 60	39.11	0.61	-6.81	0.70	1.69	1.08	2.12
Dg of M= 1.4335	**110**	75 / 60 / 58	39.23	-2.47	-8.79	0.82	-1.39	-0.90	1.85
Db of Y = 1.2408	**111**	75 / 60 / 60	39.16	-2.76	-7.49	0.75	-1.68	0.40	1.88
	112	75 / 62 / 58	38.48	-0.79	-9.17	0.07	0.29	-1.28	1.31
C^*_{ab}:	**113**	**75 / 62 / 60 ***	**38.41**	**-1.08**	**-7.89**	**0.00**	**0.00**	**0.00**	**0.00**
	114	75 / 62 / 62	38.35	-1.36	-6.60	-0.06	-0.28	1.29	1.32
min.: 6.50 (**107**)	**115**	75 / 64 / 60	37.67	0.62	-8.28	-0.74	1.70	-0.39	1.90
max.: 9.40 (**119**)	**116**	75 / 64 / 62	37.60	0.35	-7.01	-0.81	1.43	0.88	1.86
	117	77 / 62 / 60	37.72	-2.79	-8.96	-0.69	-1.71	-1.07	2.13
Illuminant: D_{50}	**118**	77 / 62 / 62	37.65	-3.09	-7.68	-0.76	-2.01	0.21	2.16
CIE Observer: 10°	**119**	77 / 64 / 60	36.98	-1.10	-9.34	-1.43	-0.02	-1.45	2.04
	120	77 / 64 / 62	36.91	-1.39	-8.08	-1.50	-0.31	-0.19	1.54
		min	36.91	-3.09	-9.34	-1.50	-2.01	-1.45	0.00
		max.	39.93	0.88	-6.41	1.52	1.96	1.48	2.16
		avg.	38.42	-1.08	-7.89	0.01	0.00	0.00	1.72
		stdev.	0.97	1.30	0.92	0.97	1.30	0.92	0.56

Note :* The C-M-Y dot area combination of the three-color overprint (aim) gray is printed at the aim SID levels.

Table C1 (continued).

SID Combination		C/M/Y (%)	L*	a*	b*	ΔL*	Δa*	Δb*	ΔE^*_{ab}
09(AAH)	**121**	73 / 60 / 58	39.54	-1.05	-6.24	1.13	0.03	1.65	2.00
	122	73 / 60 / 60	39.46	-1.33	-4.88	1.05	-0.25	3.01	3.20
SID:	**123**	73 / 62 / 58	38.80	0.55	-6.62	0.39	1.63	1.27	2.10
Dr of C = 1.4576	**124**	73 / 62 / 60	38.72	0.27	-5.27	0.31	1.35	2.62	2.96
Dg of M= 1.4335	**125**	75 / 60 / 58	38.84	-2.70	-7.32	0.43	-1.62	0.57	1.77
Db of Y = 1.3406	**126**	75 / 60 / 60	38.76	-3.00	-5.96	0.35	-1.92	1.93	2.75
	127	75 / 62 / 58	38.10	-1.10	-7.70	-0.31	-0.02	0.19	0.36
C^*_{ab}:	**128**	**75 / 62 / 60**	**38.02**	**-1.40**	**-6.35**	**-0.39**	**-0.32**	**1.54**	**1.62**
	129	75 / 62 / 62	37.94	-1.68	-5.00	-0.47	-0.60	2.89	2.99
min.: 5.06 **(122)**	**130**	75 / 64 / 60	37.29	0.22	-6.74	-1.12	1.30	1.15	2.07
max.: 8.05 **(132)**	**131**	75 / 64 / 62	37.21	-0.07	-5.41	-1.20	1.01	2.48	2.93
	132	77 / 62 / 60	37.33	-3.09	-7.43	-1.08	-2.01	0.46	2.33
Illuminant: D_{50}	**133**	77 / 62 / 62	37.25	-3.39	-6.08	-1.16	-2.31	1.81	3.16
CIE Observer: 10°	**134**	77 / 64 / 60	36.60	-1.49	-7.81	-1.81	-0.41	0.08	1.86
	135	77 / 64 / 62	36.52	-1.78	-6.48	-1.89	-0.70	1.41	2.46
		min	36.52	-3.39	-7.81	-1.89	-2.31	0.08	0.36
		max.	39.54	0.55	-4.88	1.13	1.63	3.01	3.20
		avg.	38.03	-1.40	-6.35	-0.38	-0.32	1.54	2.30
		stdev.	0.97	1.27	0.95	0.97	1.27	0.95	0.75

Note : The L*, a*, and b* values of the (aim) standard are 38.41, -1.08, and -7.89, respectively.

Table C1 (continued).

SID Combination		C/M/Y (%)	L*	a*	b*	ΔL*	Δa*	Δb*	ΔE^*_{ab}
10(AHA)	**136**	73 / 60 / 58	39.17	0.23	-7.41	0.76	1.31	0.48	1.59
	137	73 / 60 / 60	39.10	-0.05	-6.14	0.69	1.03	1.75	2.15
SID:	**138**	73 / 62 / 58	38.39	1.96	-7.78	-0.02	3.04	0.11	3.04
Dr of C = 1.4576	**139**	73 / 62 / 60	38.32	1.70	-6.52	-0.09	2.78	1.37	3.10
Dg of M= 1.5335	**140**	75 / 60 / 58	38.47	-1.42	-8.48	0.06	-0.34	-0.59	0.68
Db of Y = 1.2408	**141**	75 / 60 / 60	38.40	-1.71	-7.21	0.01	-0.63	0.68	0.93
	142	75 / 62 / 58	37.69	0.31	-8.84	-0.72	1.39	-0.95	1.83
C^*_{ab}:	**143**	**75 / 62 / 60**	**37.62**	**0.02**	**-7.59**	**-0.79**	**1.10**	**0.30**	**1.39**
	144	75 / 62 / 62	37.56	-0.25	-6.33	-0.85	0.83	1.56	1.96
min.: 6.14 **(137)**	**145**	75 / 64 / 60	36.85	1.77	-7.97	-1.56	2.85	-0.08	3.25
min.: 9.02 **(149)**	**146**	75 / 64 / 62	36.78	1.51	-6.72	-1.63	2.59	1.17	3.28
	147	77 / 62 / 60	36.94	-1.67	-8.64	-1.47	-0.59	-0.75	1.75
Illuminant: D_{50}	**148**	77 / 62 / 62	36.87	-1.96	-7.39	-1.54	-0.88	0.50	1.84
CIE Observer: 10°	**149**	77 / 64 / 60	36.17	0.08	-9.02	-2.24	1.16	-1.13	2.76
	150	77 / 64 / 62	36.10	-0.21	-7.78	-2.31	0.87	0.11	2.47
		min	36.10	-1.96	-9.02	-2.31	-0.88	-1.13	0.68
		max.	39.17	1.96	-6.14	0.76	3.04	1.75	3.28
		avg.	37.63	0.02	-7.59	-0.78	1.10	0.30	2.14
		stdev.	0.99	1.31	0.91	0.99	1.31	0.91	0.83

Note : The L*, a*, and b* values of the (aim) standard are 38.41, -1.08, and -7.89, respectively.

Table C1 (continued).

SID Combination		C/M/Y (%)	L*	a*	b*	ΔL*	Δa*	Δb*	ΔE^*_{ab}
11(AHH)	**151**	73 / 60 / 58	38.85	0.31	-6.00	0.44	1.39	1.89	2.39
	152	73 / 60 / 60	38.78	0.04	-4.67	0.37	1.12	3.22	3.43
SID:	**153**	73 / 62 / 58	38.09	1.97	-6.37	-0.32	3.05	1.52	3.42
Dr of C = 1.4576	**154**	73 / 62 / 60	38.01	1.71	-5.05	-0.40	2.79	2.84	4.00
Dg of M= 1.5335	**155**	75 / 60 / 58	38.15	-1.32	-7.07	-0.26	-0.24	0.82	0.89
Db of Y = 1.3406	**156**	75 / 60 / 60	38.07	-1.60	-5.74	-0.34	-0.52	2.15	2.24
	157	75 / 62 / 58	37.40	0.33	-7.43	-1.01	1.41	0.46	1.79
C^*_{ab}:	**158**	**75 / 62 / 60**	**37.32**	**0.06**	**-6.12**	**-1.09**	**1.14**	**1.77**	**2.37**
	159	75 / 62 / 62	37.24	-0.21	-4.80	-1.17	0.87	3.09	3.42
min.: 4.67 **(152)**	**160**	75 / 64 / 60	36.56	1.73	-6.49	-1.85	2.81	1.40	3.64
max.: 7.55 **(164)**	**161**	75 / 64 / 62	36.49	1.46	-5.19	-1.92	2.54	2.70	4.18
	162	77 / 62 / 60	36.63	-1.62	-7.18	-1.78	-0.54	0.71	1.99
Illuminant: D_{50}	**163**	77 / 62 / 62	36.55	-1.91	-5.86	-1.86	-0.83	2.03	2.88
CIE Observer: 10°	**164**	77 / 64 / 60	35.88	0.04	-7.55	-2.53	1.12	0.34	2.79
	165	77 / 64 / 62	35.80	-0.24	-6.25	-2.61	0.84	1.64	3.20
		min	35.80	-1.91	-7.55	-2.61	-0.83	0.34	0.89
		max.	38.85	1.97	-4.67	0.44	3.05	3.22	4.18
		avg.	37.32	0.05	-6.12	-1.09	1.13	1.77	2.84
		stdev.	0.98	1.28	0.93	0.98	1.28	0.93	0.90

Note : The L*, a*, and b* values of the (aim) standard are 38.41, -1.08, and -7.89, respectively.

Table C1 (continued).

SID Combination		C/M/Y (%)	L*	a*	b*	ΔL*	Δa*	Δb*	ΔE^*_{ab}
12 (HAA)	**166**	73 / 60 / 58	38.87	-0.85	-9.01	0.46	0.23	-1.12	1.23
	167	73 / 60 / 60	38.79	-1.11	-7.75	0.38	-0.03	0.14	0.41
SID:	**168**	73 / 62 / 58	38.14	0.77	-9.37	-0.27	1.85	-1.48	2.38
Dr of C = 1.5572	**169**	73 / 62 / 60	38.07	0.52	-8.12	-0.34	1.60	-0.23	1.65
Dg of M= 1.4335	**170**	75 / 60 / 58	38.13	-2.53	-10.13	-0.28	-1.45	-2.24	2.68
Db of Y = 1.2408	**171**	75 / 60 / 60	38.06	-2.80	-8.87	-0.35	-1.72	-0.98	2.01
	172	75 / 62 / 58	37.41	-0.91	-10.49	-1.00	0.17	-2.60	2.79
C^*_{ab}:	**173**	**75 / 62 / 60**	**37.33**	**-1.18**	**-9.24**	**-1.08**	**-0.10**	**-1.35**	**1.73**
	174	75 / 62 / 62	37.26	-1.44	-7.99	-1.15	-0.36	-0.10	1.21
min.: 7.83 **(167)**	**175**	75 / 64 / 60	36.61	0.46	-9.61	-1.80	1.54	-1.72	2.93
max.: 10.79 **(179)**	**176**	75 / 64 / 62	36.54	0.20	-8.37	-1.87	1.28	-0.48	2.32
	177	77 / 62 / 60	36.61	-2.90	-10.35	-1.80	-1.82	-2.46	3.55
Illuminant: D_{50}	**178**	77 / 62 / 62	36.53	-3.18	-9.11	-1.88	-2.10	-1.22	3.07
CIE Observer: 10°	**179**	77 / 64 / 60	35.89	-1.27	-10.72	-2.52	-0.19	-2.83	3.79
	180	77 / 64 / 62	35.82	-1.54	-9.49	-2.59	-0.46	-1.60	3.08
		min	35.82	-3.18	-10.72	-2.59	-2.10	-2.83	0.41
		max.	38.87	0.77	-7.75	0.46	1.85	0.14	3.79
		avg.	37.34	-1.18	-9.24	-1.07	-0.10	-1.35	2.32
		stdev.	0.98	1.28	0.93	0.98	1.28	0.93	0.95

Note : The L*, a*, and b* values of the (aim) standard are 38.41, -1.08, and -7.89, respectively.

Table C1 (continued).

SID Combination		C/M/Y (%)	L*	a*	b*	ΔL*	Δa*	Δb*	ΔE^*_{ab}
13 (HAH)	**181**	73 / 60 / 58	38.65	-1.79	-7.25	0.24	-0.71	0.64	0.99
	182	73 / 60 / 60	38.57	-2.08	-5.91	0.16	-1.00	1.98	2.22
SID:	**183**	73 / 62 / 58	37.93	-0.22	-7.61	-0.48	0.86	0.28	1.02
Dr of C = 1.5572	**184**	73 / 62 / 60	37.85	-0.49	-6.28	-0.56	0.59	1.61	1.80
Dg of M= 1.4335	**185**	75 / 60 / 58	37.92	-3.48	-8.35	-0.49	-2.40	-0.46	2.49
Db of Y = 1.3407	**186**	75 / 60 / 60	37.84	-3.78	-7.02	-0.57	-2.70	0.87	2.89
	187	75 / 62 / 58	37.20	-1.91	-8.71	-1.21	-0.83	-0.82	1.68
C^*_{ab}:	**188**	**75 / 62 / 60**	**37.12**	**-2.21**	**-7.39**	**-1.29**	**-1.13**	**0.50**	**1.79**
	189	75 / 62 / 62	37.04	-2.49	-6.07	-1.37	-1.41	1.82	2.68
min.: 6.27 **(182)**	**190**	75 / 64 / 60	36.41	-0.62	-7.76	-2.00	0.46	0.13	2.06
max.: 9.36 **(192)**	**191**	75 / 64 / 62	36.33	-0.91	-6.45	-2.08	0.17	1.44	2.54
	192	77 / 62 / 60	36.41	-3.95	-8.49	-2.00	-2.87	-0.60	3.55
Illuminant: D_{50}	**193**	77 / 62 / 62	36.33	-4.25	-7.17	-2.00	-3.17	0.72	3.86
CIE Observer: 10°	**194**	77 / 64 / 60	35.70	-2.37	-8.86	-2.71	-1.29	-0.97	3.15
	195	77 / 64 / 62	35.62	-2.67	-7.55	-2.79	-1.59	0.34	3.23
		min	35.62	-4.25	-8.86	-2.79	-3.17	-0.97	0.99
		max.	38.65	-0.22	-5.91	0.24	0.86	1.98	3.86
		avg.	37.13	-2.21	-7.39	-1.28	-1.13	0.50	2.40
		stdev.	0.98	1.28	0.94	0.98	1.28	0.94	0.86

Note : The L*, a*, and b* values of the (aim) standard are 38.41, -1.08, and -7.89, respectively.

Table C1 (continued).

SID Combination		C/M/Y (%)	L*	a*	b*	ΔL*	Δa*	Δb*	ΔE^*_{ab}
14 (HHA)	**196**	73 / 60 / 58	38.08	0.08	-8.68	-0.33	1.16	-0.79	1.44
	197	73 / 60 / 60	38.00	-0.18	-7.43	-0.41	0.90	0.46	1.09
SID:	**198**	73 / 62 / 58	37.32	1.75	-9.03	-1.09	2.83	-1.14	3.24
Dr of C = 1.5571	**199**	73 / 62 / 60	37.25	1.50	-7.79	-1.16	2.58	0.10	2.83
Dg of M= 1.5335	**200**	75 / 60 / 58	37.35	-1.59	-9.78	-1.06	-0.51	-1.89	2.23
Db of Y = 1.2408	**201**	75 / 60 / 60	37.27	-1.86	-8.54	-1.14	-0.78	-0.65	1.53
	202	75 / 62 / 58	36.60	0.08	-10.13	-1.81	1.16	-2.24	3.10
C^*_{ab}:	**203**	**75 / 62 / 60**	**36.52**	**-0.19**	**-8.90**	**-1.89**	**0.89**	**-1.01**	**2.32**
	204	75 / 62 / 62	36.45	-0.45	-7.66	-1.96	0.63	0.23	2.07
min.: 7.43 **(197)**	**205**	75 / 64 / 60	35.77	1.50	-9.25	-2.64	2.58	-1.36	3.93
max.: 10.34 **(209)**	**206**	75 / 64 / 62	35.70	1.24	-8.03	-2.71	2.32	-0.14	3.57
	207	77 / 62 / 60	35.81	-1.90	-9.99	-2.60	-0.82	-2.10	3.44
Illuminant: D_{50}	**208**	77 / 62 / 62	35.73	-2.17	-8.76	-2.68	-1.09	-0.87	3.02
CIE Observer: 10°	**209**	77 / 64 / 60	35.06	-0.22	-10.34	-3.35	0.86	-2.45	4.24
	210	77 / 64 / 62	34.99	-0.49	-9.12	-3.42	0.59	-1.23	3.68
		min	34.99	-2.17	-10.34	-3.42	-1.09	-2.45	1.09
		max.	38.08	1.75	-7.43	-0.33	2.83	0.46	4.24
		avg.	36.53	-0.19	-8.90	-1.88	0.89	-1.01	2.78
		stdev.	1.00	1.29	0.91	1.00	1.29	0.91	0.96

Note : The L*, a*, and b* values of the (aim) standard are 38.41, -1.08, and -7.89, respectively.

Table C1 (continued).

SID Combination		C/M/Y (%)	L*	a*	b*	ΔL*	Δa*	Δb*	ΔE^*_{ab}
15 (HHH)	**211**	73 / 60 / 58	37.83	-0.20	-7.33	-0.58	0.88	0.56	1.19
	212	73 / 60 / 60	37.75	-0.46	-6.02	-0.66	0.62	1.87	2.08
SID:	**213**	73 / 62 / 58	37.08	1.45	-7.69	-1.33	2.53	0.20	2.87
Dr of C = 1.5571	**214**	73 / 62 / 60	37.00	1.19	-6.40	-1.41	2.27	1.49	3.06
Dg of M= 1.5335	**215**	75 / 60 / 58	37.10	-1.86	-8.44	-1.31	-0.78	-0.55	1.62
Db of Y = 1.3406	**216**	75 / 60 / 60	37.02	-2.14	-7.14	-1.39	-1.06	0.75	1.90
	217	75 / 62 / 58	36.36	-0.23	-8.80	-2.05	0.85	-0.91	2.40
C^*_{ab}:	**218**	**75 / 62 / 60**	**36.28**	**-0.50**	**-7.51**	**-2.13**	**0.58**	**0.38**	**2.24**
	219	75 / 62 / 62	36.20	-0.76	-6.22	-2.21	0.32	1.67	2.79
min.: 6.04 (**212**)	**220**	75 / 64 / 60	35.53	1.16	-7.88	-2.88	2.24	0.01	3.65
max.: 9.00 (**224**)	**221**	75 / 64 / 62	35.45	0.90	-6.61	-2.96	1.98	1.28	3.78
	222	77 / 62 / 60	35.56	-2.21	-8.61	-2.85	-1.13	-0.72	3.15
Illuminant: D_{50}	**223**	77 / 62 / 62	35.48	-2.48	-7.33	-2.93	-1.40	0.56	3.30
CIE Observer: 10°	**224**	77 / 64 / 60	34.82	-0.56	-8.98	-3.59	0.52	-1.09	3.79
	225	77 / 64 / 62	34.74	-0.83	-7.71	-3.67	0.25	0.18	3.68
		min	34.74	-2.48	-8.98	--3.67	-1.40	-1.09	1.19
		max.	37.83	1.45	-6.02	-0.58	2.53	1.87	3.79
		avg.	36.28	-0.50	-7.51	-2.13	0.58	0.38	2.77
		stdev.	1.00	1.28	0.93	1.00	1.28	0.93	0.83

Note : The L*, a*, and b* values of the (aim) standard are 38.41, -1.08, and -7.89, respectively.

Table C2. Status E densities of the 225 three-color overprint halftone grays printed at 15 C-M-Y combinations of SIDs and of dot areas according to the FIPP SID and dot gain specifications

	Dot Areas of C/M/Y	01(LLL)			02(LLA)			03(LAL)		
		D_r	D_g	D_b	D_r	D_g	D_b	D_r	D_g	D_b
1	73 / 60 / 58	0.8637	0.8395	0.8582	0.8626	0.8458	0.8866	0.8714	0.8611	0.8726
2	73 / 60 / 60	0.8638	0.8411	0.8784	0.8627	0.8476	0.9084	0.8714	0.8626	0.8925
3	73 / 62 / 58	0.8665	0.8625	0.8672	0.8652	0.8689	0.8956	0.8743	0.8855	0.8823
4	73 / 62 / 60	0.8665	0.8641	0.8873	0.8652	0.8707	0.9173	0.8744	0.8870	0.9021
5	75 / 60 / 58	0.8965	0.8459	0.8601	0.8953	0.8522	0.8885	0.9042	0.8675	0.8745
6	75 / 60 / 60	0.8966	0.8475	0.8802	0.8953	0.8541	0.9103	0.9042	0.8689	0.8944
7	75 / 62 / 58	0.8992	0.8688	0.8691	0.8978	0.8752	0.8974	0.9071	0.8917	0.8841
8	**75 / 62 / 60**	0.8993	0.8704	0.8891	0.8978	0.8771	0.9191	0.9072	0.8931	0.9039
9	75 / 62 / 62	0.8993	0.8720	0.9096	0.8978	0.8789	0.9412	0.9072	0.8946	0.9240
10	75 / 64 / 60	0.9020	0.8939	0.8981	0.9004	0.9007	0.9280	0.9102	0.9180	0.9135
11	75 / 64 / 62	0.9020	0.8955	0.9185	0.9004	0.9025	0.9501	0.9102	0.9195	0.9335
12	77 / 62 / 60	0.9332	0.8767	0.8909	0.9316	0.8834	0.9209	0.9412	0.8993	0.9057
13	77 / 62 / 62	0.9332	0.8783	0.9113	0.9316	0.8852	0.9430	0.9412	0.9008	0.9258
14	77 / 64 / 60	0.9359	0.9000	0.8999	0.9341	0.9069	0.9298	0.9441	0.9241	0.9153
15	77 / 64 / 62	0.9359	0.9017	0.9202	0.9341	0.9088	0.9518	0.9441	0.9256	0.9353

Table C2 (continued).

	Dot Areas of C/M/Y	04(LAA)			05(ALL)			06(ALA)		
		D_r	D_g	D_b	D_r	D_g	D_b	D_r	D_g	D_b
1	73 / 60 / 58	0.8646	0.8717	0.9008	0.9034	0.8522	0.8674	0.9059	0.8526	0.8974
2	73 / 60 / 60	0.8644	0.8735	0.9223	0.9035	0.8536	0.8875	0.9061	0.8541	0.9192
3	73 / 62 / 58	0.8672	0.8964	0.9104	0.9062	0.8749	0.8763	0.9085	0.8757	0.9063
4	73 / 62 / 60	0.8671	0.8982	0.9318	0.9063	0.8763	0.8964	0.9087	0.8772	0.9280
5	75 / 60 / 58	0.8972	0.8782	0.9027	0.9389	0.8590	0.8695	0.9415	0.8592	0.8996
6	75 / 60 / 60	0.8971	0.8800	0.9242	0.9390	0.8604	0.8896	0.9416	0.8607	0.9241
7	75 / 62 / 58	0.8998	0.9028	0.9123	0.9417	0.8816	0.8784	0.9440	0.8822	0.9084
8	**75 / 62 / 60**	0.8997	0.9046	0.9336	0.9417	0.8830	0.8984	0.9442	0.8837	0.9301
9	75 / 62 / 62	0.8995	0.9065	0.9554	0.9418	0.8844	0.9188	0.9443	0.8852	0.9523
10	75 / 64 / 60	0.9023	0.9299	0.9432	0.9445	0.9062	0.9073	0.9467	0.9073	0.9390
11	75 / 64 / 62	0.9021	0.9318	0.9649	0.9446	0.9076	0.9276	0.9468	0.9088	0.9610
12	77 / 62 / 60	0.9335	0.9110	0.9355	0.9786	0.8897	0.9005	0.9811	0.8902	0.9322
13	77 / 62 / 62	0.9333	0.9129	0.9572	0.9786	0.8911	0.9208	0.9812	0.8917	0.9543
14	77 / 64 / 60	0.9360	0.9362	0.9450	0.9813	0.9127	0.9093	0.9836	0.9137	0.9410
15	77 / 64 / 62	0.9358	0.9381	0.9667	0.9814	0.9141	0.9296	0.9837	0.9152	0.9631

Table C2 (continued).

	Dot Areas of C/M/Y	07(AAL)			08(AAA)			09(AAH)		
		D_r	D_g	D_b	D_r	D_g	D_b	D_r	D_g	D_b
1	73 / 60 / 58	0.9146	0.8775	0.8791	0.9098	0.8784	0.9085	0.9191	0.8878	0.9345
2	73 / 60 / 60	0.9147	0.8789	0.8990	0.9097	0.8798	0.9301	0.9192	0.8896	0.9576
3	73 / 62 / 58	0.9178	0.9017	0.8885	0.9126	0.9031	0.9179	0.9223	0.9120	0.9439
4	73 / 62 / 60	0.9179	0.9031	0.9084	0.9124	0.9046	0.9394	0.9224	0.9137	0.9669
5	75 / 60 / 58	0.9504	0.8843	0.8812	0.9456	0.8851	0.9107	0.9547	0.8947	0.9366
6	75 / 60 / 60	0.9504	0.8857	0.9011	0.9454	0.8865	0.9323	0.9549	0.8964	0.9597
7	75 / 62 / 58	0.9535	0.9084	0.8906	0.9482	0.9097	0.9200	0.9579	0.9187	0.9459
8	**75 / 62 / 60**	0.9536	0.9098	0.9104	0.9481	0.9111	0.9415	0.9581	0.9204	0.9689
9	75 / 62 / 62	0.9536	0.9112	0.9306	0.9480	0.9126	0.9634	0.9582	0.9222	0.9925
10	75 / 64 / 60	0.9568	0.9346	0.9198	0.9508	0.9364	0.9508	0.9613	0.9451	0.9783
11	75 / 64 / 62	0.9568	0.9360	0.9399	0.9506	0.9379	0.9727	0.9614	0.9469	1.0017
12	77 / 62 / 60	0.9907	0.9165	0.9124	0.9852	0.9177	0.9436	0.9951	0.9272	0.9709
13	77 / 62 / 62	0.9907	0.9179	0.9326	0.9850	0.9191	0.9655	0.9952	0.9289	0.9945
14	77 / 64 / 60	0.9939	0.9411	0.9217	0.9878	0.9428	0.9528	0.9983	0.9517	0.9803
15	77 / 64 / 62	0.9939	0.9425	0.9418	0.9877	0.9443	0.9747	0.9984	0.9535	1.0037

Table C2 (continued).

	Dot Areas of C/M/Y	10(AHA)			11(AHH)			12(HAA)		
		D_r	D_g	D_b	D_r	D_g	D_b	D_r	D_g	D_b
1	73 / 60 / 58	0.9186	0.9006	0.9297	0.9208	0.9103	0.9547	0.9372	0.9024	0.9196
2	73 / 60 / 60	0.9188	0.9020	0.9510	0.9210	0.9120	0.9775	0.9370	0.9042	0.9408
3	73 / 62 / 58	0.9217	0.9267	0.9399	0.9241	0.9358	0.9650	0.9398	0.9268	0.9290
4	73 / 62 / 60	0.9218	0.9282	0.9612	0.9243	0.9376	0.9877	0.9397	0.9286	0.9502
5	75 / 60 / 58	0.9540	0.9073	0.9320	0.9560	0.9172	0.9569	0.9748	0.9099	0.9220
6	75 / 60 / 60	0.9541	0.9087	0.9533	0.9562	0.9189	0.9798	0.9746	0.9117	0.9432
7	75 / 62 / 58	0.9570	0.9333	0.9422	0.9592	0.9426	0.9672	0.9774	0.9342	0.9315
8	**75 / 62 / 60**	0.9571	0.9347	0.9635	0.9594	0.9444	0.9899	0.9772	0.9359	0.9526
9	75 / 62 / 62	0.9573	0.9362	0.9852	0.9596	0.9461	1.0132	0.9771	0.9377	0.9742
10	75 / 64 / 60	0.9601	0.9615	0.9738	0.9626	0.9705	1.0002	0.9799	0.9609	0.9620
11	75 / 64 / 62	0.9602	0.9630	0.9954	0.9629	0.9723	1.0233	0.9797	0.9627	0.9835
12	77 / 62 / 60	0.9938	0.9413	0.9658	0.9959	0.9511	0.9921	1.0164	0.9433	0.9550
13	77 / 62 / 62	0.9940	0.9428	0.9875	0.9961	0.9529	1.0154	1.0162	0.9451	0.9765
14	77 / 64 / 60	0.9967	0.9680	0.9760	0.9991	0.9772	1.0024	1.0190	0.9681	0.9643
15	77 / 64 / 62	0.9969	0.9694	0.9976	0.9993	0.9789	1.0255	1.0188	0.9699	0.9858

Table C2 (continued).

	Dot Areas of C/M/Y	13(HAH)			14(HHA)			15(HHH)		
		D_r	D_g	D_b	D_r	D_g	D_b	D_r	D_g	D_b
1	73 / 60 / 58	0.9473	0.9035	0.9465	0.9477	0.9244	0.9378	0.9528	0.9317	0.9634
2	73 / 60 / 60	0.9474	0.9053	0.9694	0.9478	0.9262	0.9589	0.9530	0.9337	0.9860
3	73 / 62 / 58	0.9503	0.9274	0.9560	0.9508	0.9502	0.9480	0.9560	0.9574	0.9737
4	73 / 62 / 60	0.9504	0.9292	0.9788	0.9508	0.9519	0.9691	0.9562	0.9594	0.9962
5	75 / 60 / 58	0.9849	0.9109	0.9489	0.9851	0.9319	0.9403	0.9902	0.9393	0.9660
6	75 / 60 / 60	0.9850	0.9127	0.9717	0.9852	0.9337	0.9614	0.9904	0.9413	0.9885
7	75 / 62 / 58	0.9879	0.9347	0.9584	0.9881	0.9576	0.9506	0.9934	0.9649	0.9761
8	**75 / 62 / 60**	0.9880	0.9365	0.9811	0.9881	0.9593	0.9715	0.9936	0.9668	0.9986
9	75 / 62 / 62	0.9882	0.9382	1.0043	0.9882	0.9611	0.9930	0.9938	0.9688	1.0216
10	75 / 64 / 60	0.9910	0.9608	0.9905	0.9911	0.9857	0.9818	0.9967	0.9931	1.0088
11	75 / 64 / 62	0.9912	0.9626	1.0137	0.9911	0.9875	1.0031	0.9969	0.9951	1.0317
12	77 / 62 / 60	1.0272	0.9437	0.9834	1.0271	0.9667	0.9740	1.0325	0.9743	1.0010
13	77 / 62 / 62	1.0274	0.9455	1.0066	1.0271	0.9685	0.9954	1.0327	0.9763	1.0240
14	77 / 64 / 60	1.0302	0.9679	0.9928	1.0300	0.9930	0.9842	1.0356	1.0004	1.0112
15	77 / 64 / 62	1.0303	0.9697	1.0159	1.0300	0.9947	1.0055	1.0358	1.0024	1.0340

Table C3. The L*, a*, and b* data corresponding to the Status E SIDs of cyan, magenta, and yellow inks in each C-M-Y SID combination

Combination	Solid Ink Density			Colorimetric Data		
	D_r of C	D_g of M	D_b of Y	L*	a*	b*
01(LLL)	1.3578	1.3335	1.1409	**CIELAB of Cyan SID**		
				56.7310	-35.9006	-56.8617
				CIELAB of Magenta SID		
				53.7187	80.9199	-5.0755
				CIELAB of Yellow SID		
				95.6736	-5.4655	88.6557
02(LLA)	1.3577	1.3335	1.2408	**CIELAB of Cyan SID**		
				56.7342	-35.8964	-56.8602
				CIELAB of Magenta SID		
				53.7187	80.9199	-5.0755
				CIELAB of Yellow SID		
				95.0544	-4.9574	92.4148
03(LAL)	1.3577	1.4335	1.1409	**CIELAB of Cyan SID**		
				56.7342	-35.8964	-56.8602
				CIELAB of Magenta SID		
				52.3422	82.0271	-2.6132
				CIELAB of Yellow SID		
				95.6736	-5.4655	88.6557
04(LAA)	1.3577	1.4335	1.2408	**CIELAB of Cyan SID**		
				56.7342	-35.8964	-56.8602
				CIELAB of Magenta SID		
				52.3422	82.0271	-2.6132
				CIELAB of Yellow SID		
				95.0544	-4.9574	92.4148

Table C3 (continued).

Combination	Solid Ink Density			Colorimetric Data		
	D_r of C	D_g of M	D_b of Y	L*	a*	b*
05(ALL)	1.4576	1.3335	1.1409	**CIELAB of Cyan SID**		
				54.8719	-35.6164	-58.0795
				CIELAB of Magenta SID		
				53.7187	80.9199	-5.0755
				CIELAB of Yellow SID		
				95.6736	-5.4655	88.6557
06(LLA)	1.3577	1.3335	1.2408	**CIELAB of Cyan SID**		
				56.7342	-35.8964	-56.8602
				CIELAB of Magenta SID		
				53.7187	80.9199	-5.0755
				CIELAB of Yellow SID		
				95.0544	-4.9574	92.4148
07(LAL)	1.3577	1.4335	1.1409	**CIELAB of Cyan SID**		
				56.7342	-35.8964	-56.8602
				CIELAB of Magenta SID		
				52.3422	82.0271	-2.6132
				CIELAB of Yellow SID		
				95.6736	-5.4655	88.6557
08(AAA)	1.4576	1.4335	1.2408	**CIELAB of Cyan SID**		
				54.8719	-35.6164	-58.0795
				CIELAB of Magenta SID		
				52.3422	82.0271	-2.6132
				CIELAB of Yellow SID		
				95.0544	-4.9574	92.4148

Table C3 (continued).

Combination	Solid Ink Density			Colorimetric Data
	Dr of C	Dg of M	Db of Y	L* a* b*
09(AAH)	1.4576	1.4335	1.3406	**CIELAB of Cyan SID** 54.8719 -35.6164 -58.0795 **CIELAB of Magenta SID** 52.3422 82.0271 -2.6132 **CIELAB of Yellow SID** 94.4436 -4.4186 95.7745
10(AHA)	1.4576	1.5335	1.2408	**CIELAB of Cyan SID** 54.8719 -35.6164 -58.0795 **CIELAB of Magenta SID** 51.1047 82.8326 -0.0858 **CIELAB of Yellow SID** 95.0544 -4.9574 92.4148
11(AHH)	1.4576	1.5335	1.3406	**CIELAB of Cyan SID** 54.8719 -35.6164 -58.0795 **CIELAB of Magenta SID** 51.1047 82.8326 -0.0858 **CIELAB of Yellow SID** 94.4436 -4.4186 95.7745
12(HAA)	1.5571	1.4335	1.2408	**CIELAB of Cyan SID** 53.1244 -35.1403 -59.1273 **CIELAB of Magenta SID** 52.3422 82.0271 -2.6132 **CIELAB of Yellow SID** 95.0544 -4.9574 92.4148

Table C3 (continued).

Combination	Solid Ink Density			Colorimetric Data
	D_r of C	D_g of M	D_b of Y	L* a* b*
13(HAH)	1.5571	1.4335	1.3406	**CIELAB of Cyan SID** 53.1244 -35.1403 -59.1273 **CIELAB of Magenta SID** 52.3422 82.0271 -2.6132 **CIELAB of Yellow SID** 94.4431 -4.4191 95.7732
14(HHA)	1.5571	1.5335	1.2408	**CIELAB of Cyan SID** 53.1244 -35.1403 -59.1273 **CIELAB of Magenta SID** 51.1047 82.8326 -0.0858 **CIELAB of Yellow SID** 95.0544 -4.9574 92.4148
15(HHH)	1.5571	1.5335	1.3406	**CIELAB of Cyan SID** 53.1240 -35.1383 -59.1288 **CIELAB of Magenta SID** 51.1047 82.8326 -0.0858 **CIELAB of Yellow SID** 94.4436 -4.4186 95.7745

Appendix D

The Outcomes of TWOWAY Analyses on the L*, a*, b*, and ΔE^*_{ab} Data

```
MTB  > TWOWAY C1 C2 C3;
SUBC > MEAN C2 C3.
```

Table D1. Analysis of Variance on L*

SOURCE	DF	SS	MS	F-TEST	F-CRITICAL
DOT AREA	14	356.3884	25.4563	63640.75	1.7425*
SID	14	198.2803	14.1629	35407.25	2.1739**
ERROR	196	0.0753	0.0004		
TOTAL	224	554.7440			

Note: * is F-CRITICAL at 95% confidence level
** is F-CRITICAL at 99% confidence level

Dot Area	Mean	Stdev
1	40.4080	0.946
2	40.1600	0.950
3	39.5833	0.961
4	39.3573	0.966
5	39.3747	0.954
6	39.2640	0.957
7	38.4507	0.971
8	38.4160	0.974
9	38.0253	0.972
10	37.6287	0.991
11	37.3213	0.983
12	37.3373	0.984
13	37.1280	0.976
14	36.5267	0.996
15	36.2800	0.995

POOLED STDEV = 0.972

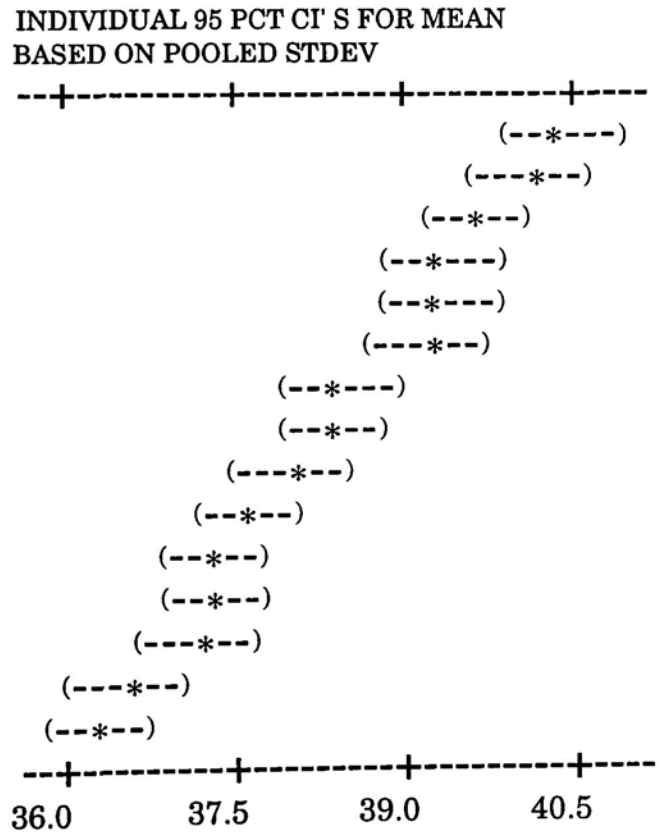

SID	Mean	Stdev
1	39.863	1.278
2	39.789	1.280
3	39.120	1.285
4	39.047	1.286
5	39.161	1.296
6	39.085	1.297
7	38.421	1.301
8	38.346	1.303
9	38.274	1.304
10	37.610	1.310
11	37.538	1.311
12	37.655	1.318
13	37.580	1.320
14	36.923	1.326
15	36.849	1.326

POOLED STDEV = 1.303

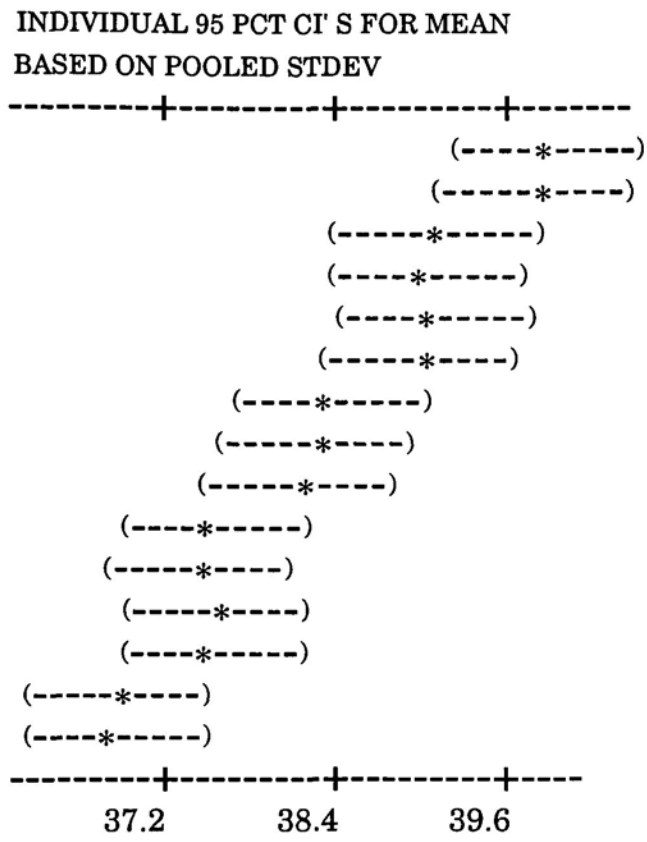

```
MTB > TWOWAY C1 C2 C3;
SUBC > MEAN C2 C3.
```

Table D2. Analysis of Variance on a*

SOURCE	DF	SS	MS	F-TEST	F-CRITICAL
DOT AREA	14	264.5493	18.8964	5905.125	1.7425*
SID	14	336.7108	24.0508	7515.875	2.1739**
ERROR	196	0.6325	0.0032		
TOTAL	224	601.8925			

Note: * is F-CRITICAL at 95% confidence level
** is F-CRITICAL at 99% confidence level

Dot Area	Mean	Stdev
1	–0.647	1.217
2	–0.491	1.223
3	0.602	1.237
4	1.357	1.245
5	–2.281	1.245
6	–2.862	1.282
7	–0.914	1.261
8	–1.083	1.301
9	–1.403	1.268
10	0.021	1.309
11	0.050	1.276
12	–1.184	1.284
13	–2.215	1.282
14	–0.193	1.293
15	–0.502	1.285

POOLED STDEV = 1.267

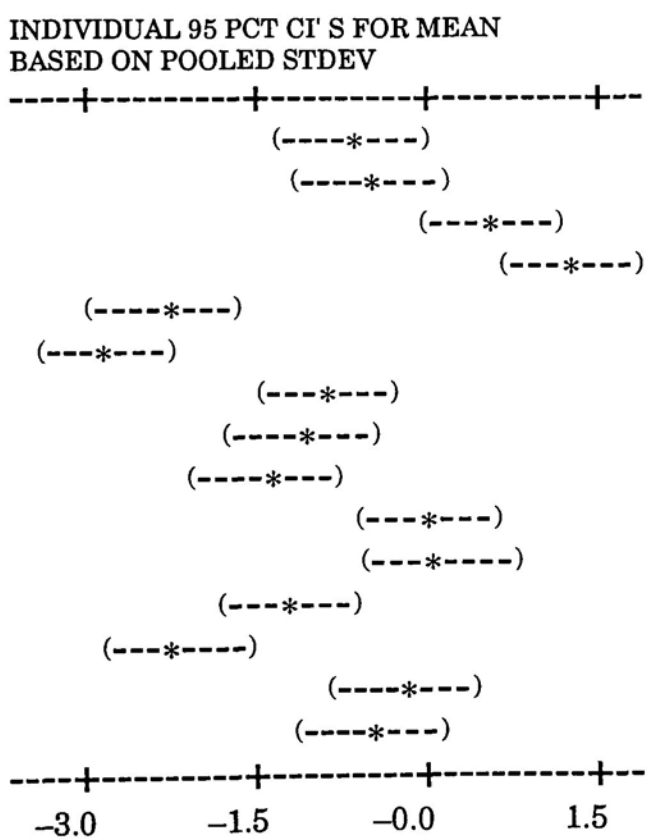

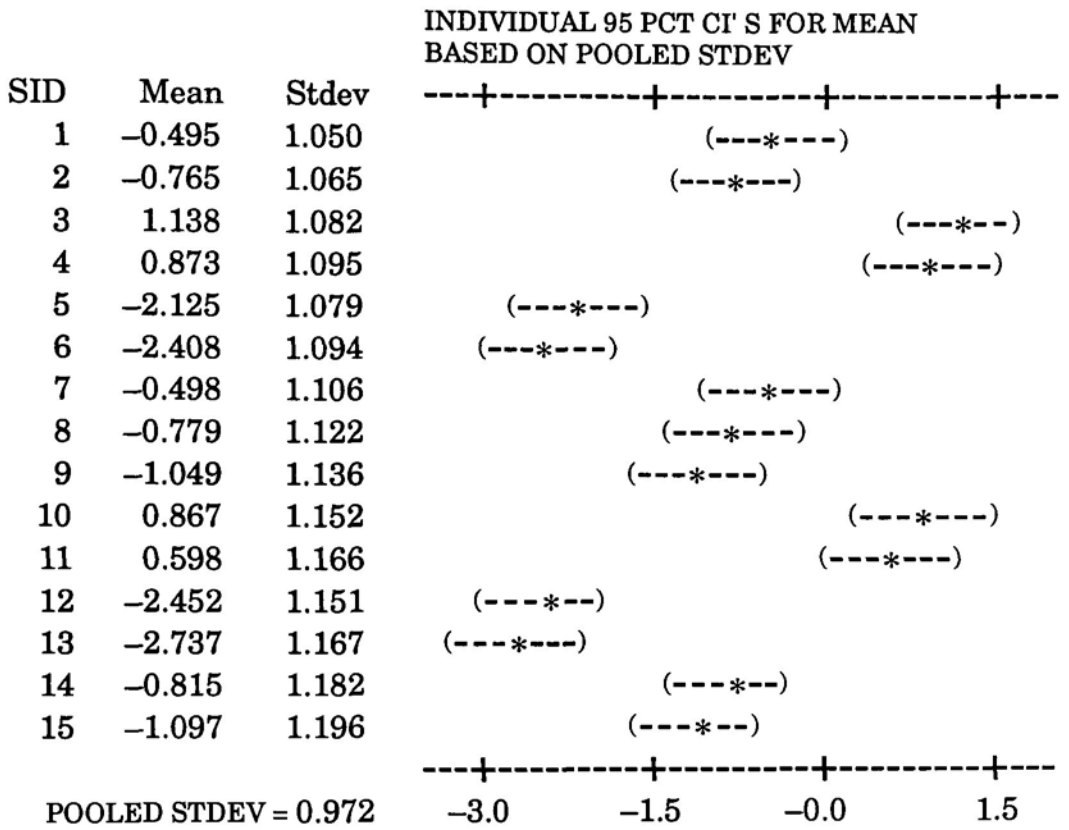
INDIVIDUAL 95 PCT CI' S FOR MEAN
BASED ON POOLED STDEV
SID Mean Stdev
1 –0.495 1.050
2 –0.765 1.065
3 1.138 1.082
4 0.873 1.095
5 –2.125 1.079
6 –2.408 1.094
7 –0.498 1.106
8 –0.779 1.122
9 –1.049 1.136
10 0.867 1.152
11 0.598 1.166
12 –2.452 1.151
13 –2.737 1.167
14 –0.815 1.182
15 –1.097 1.196
POOLED STDEV = 0.972
–3.0
–1.5
–0.0
1.5

```
MTB > TWOWAY C1 C2 C3;
SUBC > MEAN C2 C3.
```

Table D3. TWOWAY Analysis of Variance on b*

SOURCE	DF	SS	MS	F-TEST	F-CRITICAL
DOT AREA	14	271.3525	19.3823	19382.3	1.7425*
SID	14	177.4595	12.6757	12675.7	2.1739**
ERROR	196	0.2010	0.0010		
TOTAL	224	449.0131			

Note: * is F-CRITICAL at 95% confidence level
** is F-CRITICAL at 99% confidence level

Dot Area	Mean	Stdev
1	–8.591	0.901
2	–6.729	0.929
3	–8.537	0.888
4	–7.034	0.917
5	–9.553	0.906
6	–7.650	0.932
7	–9.753	0.897
8	–7.887	0.924
9	–6.353	0.948
10	–7.588	0.907
11	–6.118	0.929
12	–9.241	0.926
13	–7.391	0.945
14	–8.895	0.911
15	–7.511	0.935

POOLED STDEV = 0.920

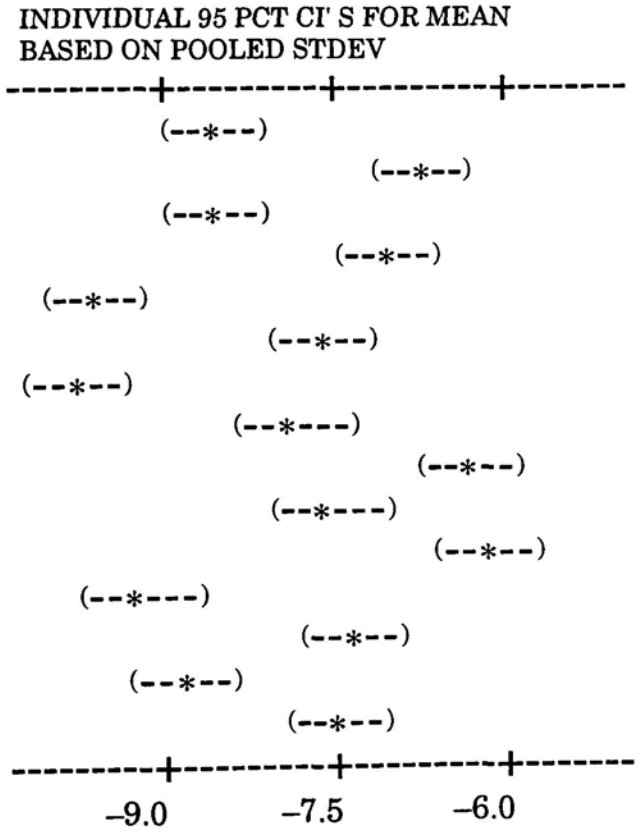

SID	Mean	Stdev
1	–7.752	1.106
2	–6.460	1.140
3	–8.120	1.098
4	–6.841	1.133
5	–8.831	1.109
6	–7.545	1.145
7	–9.197	1.103
8	–7.922	1.137
9	–6.645	1.172
10	–8.297	1.130
11	–7.035	1.163
12	–8.993	1.140
13	–7.722	1.177
14	–9.365	1.133
15	–8.106	1.168

POOLED STDEV = 1.137

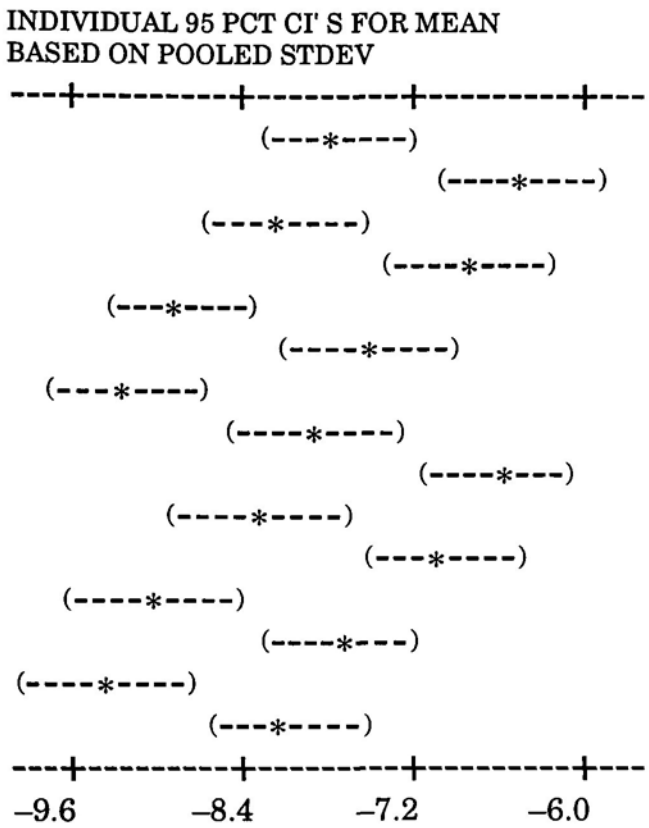

```
MTB > TWOWAY C1 C2 C3;
SUBC > MEAN C2 C3.
```

Table D4. TWOWAY Analysis of Variance on ΔE*

SOURCE	DF	SS	MS	F-TEST	F-CRITICAL
DOT AREA	14	22.461	1.604	2.089	1.7425*
SID	14	15.978	1.141	1.486	2.1739**
ERROR	196	150.571	0.768		
TOTAL	224	189.009			

Note: * is F-CRITICAL at 95% confidence level
** is F-CRITICAL at 99% confidence level

Dot Area	Mean	Stdev
1	2.6687	0.7500
2	2.6180	1.0088
3	2.6180	0.9264
4	3.0593	1.1861
5	2.7327	0.8868
6	2.4860	1.0259
7	2.4620	0.7699
8	1.7240	0.5571
9	2.3040	0.7545
10	2.1347	0.8275
11	2.8420	0.9003
12	2.3220	0.9450
13	2.3967	0.8595
14	2.7820	0.9610
15	2.7667	0.8303

POOLED STDEV = 0.8906

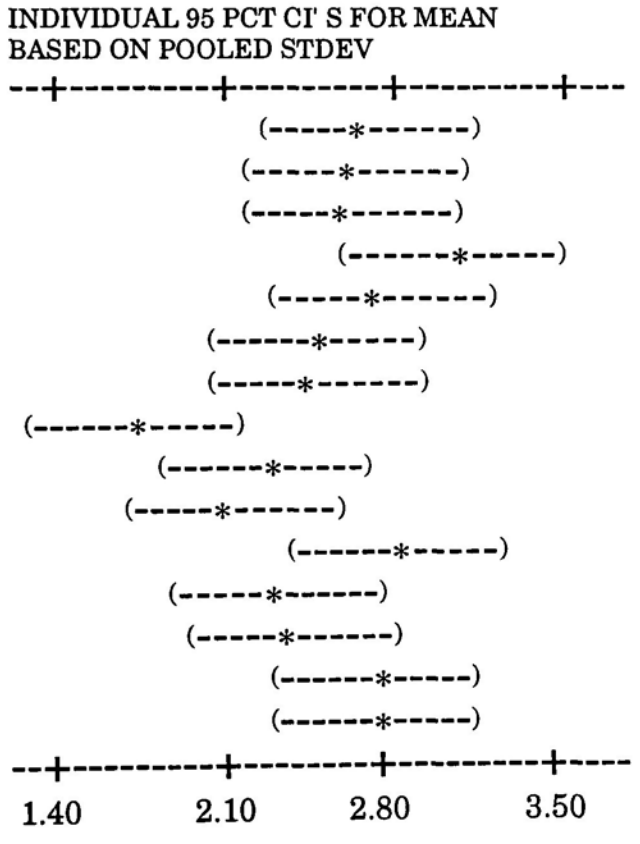

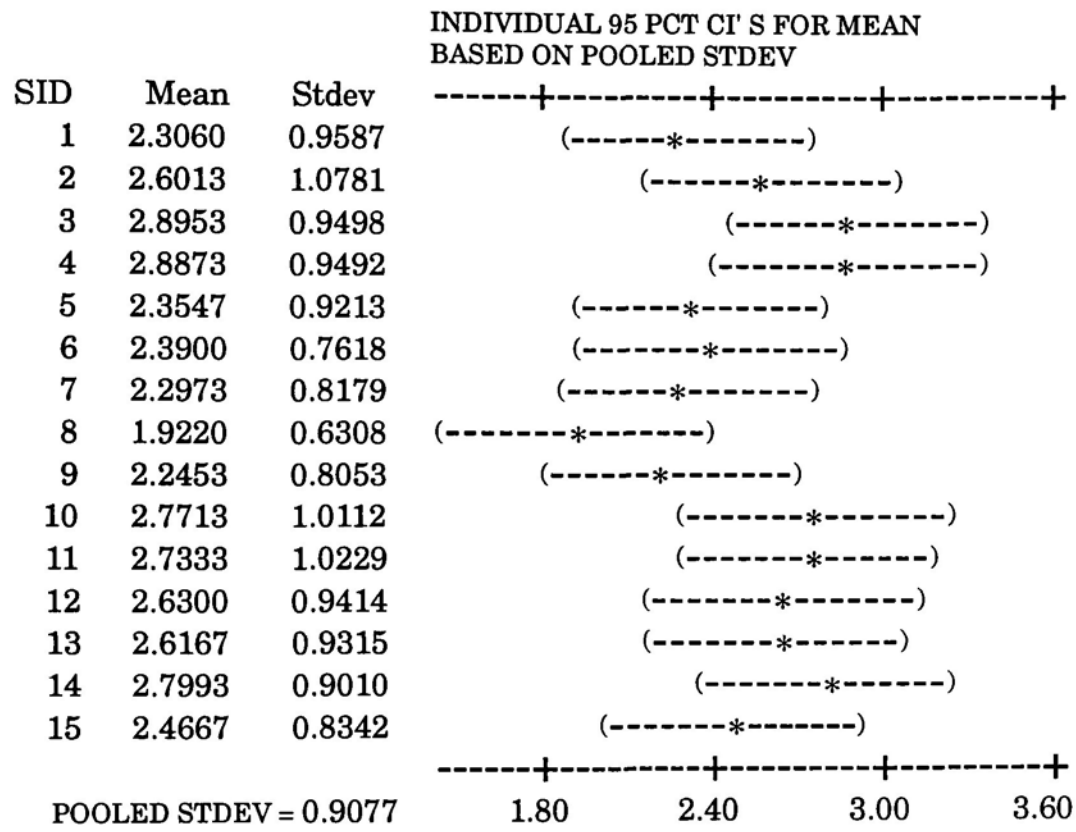
INDIVIDUAL 95 PCT CI' S FOR MEAN
BASED ON POOLED STDEV
SID Mean Stdev
1 2.3060 0.9587
2 2.6013 1.0781
3 2.8953 0.9498
4 2.8873 0.9492
5 2.3547 0.9213
6 2.3900 0.7618
7 2.2973 0.8179
8 1.9220 0.6308
9 2.2453 0.8053
10 2.7713 1.0112
11 2.7333 1.0229
12 2.6300 0.9414
13 2.6167 0.9315
14 2.7993 0.9010
15 2.4667 0.8342
POOLED STDEV = 0.9077
1.80
2.40
3.00
3.60

Vita

The author, Theera Tangvichachan, was born on February 24, 1966, in Bangkok, Thailand. After acquiring a B.Sc. in Photographic Science and Printing Technology from the Faculty of Science, Chulalongkorn University, he won a scholarship of the Royal Thai Government to pursue M.Sc. and Ph.D. degrees in Printing Technology. While waiting for admission to R.I.T., he served as an instructor at Chulalongkorn University. He will serve as professor at Sukhothaidhammathiraj University after graduation from R.I.T.